I- Supporting Experimental Section

Chemicals and reagents were purchased from Sigma-Aldrich or Fisher Scientific and were used without further purification unless otherwise stated. All solvents used were of ACS grade or higher and purchased from Fisher Chemical. The pET28a *E. coli* expression vector was purchased from Novagen. *E. coli* DH5α and BL21(DE3) competent cells were purchased from New England Biolabs. All DNA sequencing was conducted with the primers T7 promoter (5′-TAATACGACTCACTATAGGG-3′) and T7 terminator (5′-GCTAGTTATTGCTCAGCGG-3′) obtained from Integrated DNA Technologies. Nucleic acid sequencing was performed at Retrogen, Inc (San Diego, California) or ACGT, Inc (Wheeling, Illinois). Gene analysis and alignments were performed using Geneious 11.1.5. All protein structures analysis were illustrated using Molsoft ICM64. The 6DMATSsa and 6DMATSsv homology models were generated using SWISS-MODEL. Analytical TLC was performed on silica gel aluminum TLC plates purchased from Sigma-Aldrich. Visualization was accomplished with UV light (254 nm), staining with potassium permanganate solution or phosphomolybdic acid reagent and heating. Dimethylallyl pyrophosphate was purified by gravity column chromatography using silica gel (Silicycle) 60–100 or 100–200 mesh. PD-10 columns and Ni-NTA super flow columns were purchased from GE Healthcare. The NMR spectra were recorded at a 400 MHz for ^{1}H, 100 MHz for ^{13}C and 162 MHz for ^{31}P using Bruker NMR spectrometer (Chapman University School of Pharmacy Nuclear Magnetic Resonance facility) and the one-dimensional ^{1}H, ^{13}C and ^{31}P as well as two-dimensional ^{1}H-^{1}H COSY, ^{1}H-^{13}C HSQC, ^{1}H-^{13}C HMBC and ^{1}H-^{1}H NOESY spectra were recorded at ambient temperature (~25 °C) using 99.8% d_6-DMSO and D_2O obtained from Cambridge Isotope Laboratories as solvents for Trp-analogs and pyrophosphate substrates, respectively. Chemical shifts were referenced and calibrated to internal solvent resonances (DMSO, δ_H 2.50 ppm, δ_C 39.52 ppm; D_2O, δ_H 4.79 ppm) and are reported in parts per million (ppm) with coupling constants J given in Hz. The following abbreviations were used to explain the multiplicities: s = singlet, d = doublet, t = triplet, q = quartet, m = multiplet. Spectra were processed with MestreNova (Mestrelab Research).

High Performance Liquid Chromatography (HPLC) analysis were performed using a Shimadzu HPLC LCMS-2020 equipped with a diode array detector SPD-M20A (HPLC methods A and B). Purification of derivatives of Tryptophan was performed on Shimadzu (Model CBM-20A) equipped with a diode array detector SPD-M40 (HPLC methods C) and Hitachi HPLC equipped with a diode array detector L-2455 (HPLC methods D). Signals were detected at λ = 230, 254, 280 nm. Low resolution (LR) and high resolution (HR)-ESI-MS experiments were carried out using Bruker Impact II Ultra High Resolution Qq-Time-Of-Flight mass spectrometry in the positive and negative mode equipped with Thermo Scientific DIONEX 3000 UHPLC (HPLC method E).

HPLC Method A: Ascentis™ C18 (5 μm, 250 mm × 4.6 mm) column (Supelco) [25% B for 8 min, gradient of 25% B to 70% B over 40 min, 100% B for 5 min, 100% B to 25% B over 0.5 min, 25% B for 7 min (A = Milli-Q grade H_2O with 0.1% formic acid; B = Methanol with 0.1% formic acid, flow rate = 1.0 mL min^{-1};$A_{220, 254, 280}$)].

HPLC Method B: Ascentis™ C18 (5 μm, 250 mm × 4.6 mm) column (Supelco) [7% B for 3 min, gradient of 7% B to 100% B over 14 min, 100% B for 3 min, 100% B to 7% B over 0.1 min, 7% B for 5 min (A = Milli-Q grade H_2O with 0.1% formic acid; B = acetonitrile with 0.1% formic acid, flow rate = 1.0 mL min^{-1}; $A_{220, 254, 280}$)].

HPLC Method C: Ascentis™ C18 (5 μm, 250 mm × 10 mm) column (Supelco) [15% B for 10 min, gradient of 15% B to 45% B over 45 min, 45 to 100% B for 0.5 min, 100% B for 5 min, 100% B to 15% B over 0.5 min, 15% B for 7.5 min (A = Milli-Q grade H_2O with 0.1% trifluoroacetic acid; B = acetonitrile with 0.1% trifluoroacetic acid, flow rate = 4.0 mL min^{-1}; A_{280})].

HPLC Method D: Ascentis™ C18 (5 μm, 250 mm × 10 mm) column (Supelco) 15% B for 10 min, gradient of 15% B to 45% B over 45 min, 45 to 100% B for 0.5 min, 100% B for 7 min, 100% B to 15% B over 0.5 min, 15% B for 7.5 min (A = Milli-Q grade H_2O with 0.1% formic acid; B = Methanol with 0.1% formic acid, flow rate = 4.0 mL min^{-1}; A_{280})].

HPLC Method E: Titan™ C18 80 Å (1.9 μm, 50 mm × 2.1 mm) column (Supelco) [7% B for 2 min, gradient of 7% B to 100% B over 8 min, 100% B for 2 min, 100% B to 7% B over 0.5 min, 7% B for 2.5 min (A = Milli-Q grade H_2O with 0.1% formic acid; B = acetonitrile with 0.1% formic acid, flow rate = 0.3 mL min^{-1}; A_{280})].

II-Supporting Figures

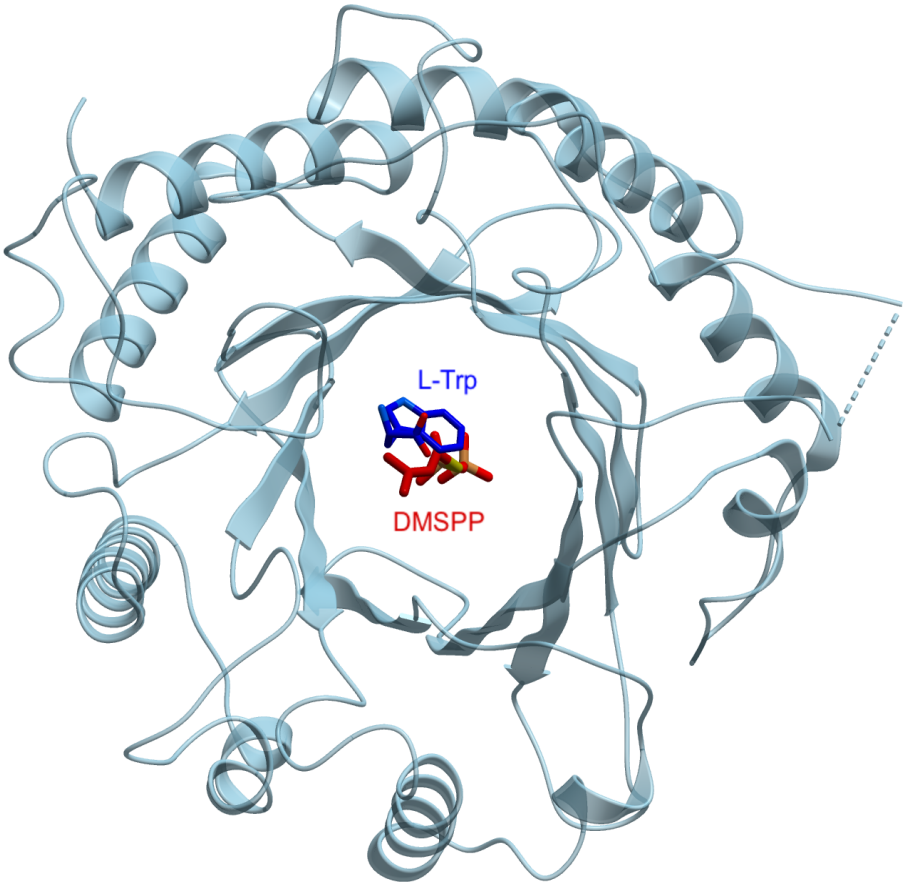

Figure S1. Overall X-ray crystal structure of ligand-bound PriB (PDB ID 5INJ) previously reported.[1] Protein structure depicted in cartoon representation. The ligands are illustrated as ball-and-stick models with the following color code: carbon, dark blue (L-Trp) and red (DMSPP); oxygen, light red; nitrogen, light blue; phosphorous, orange; sulfur, yellow.

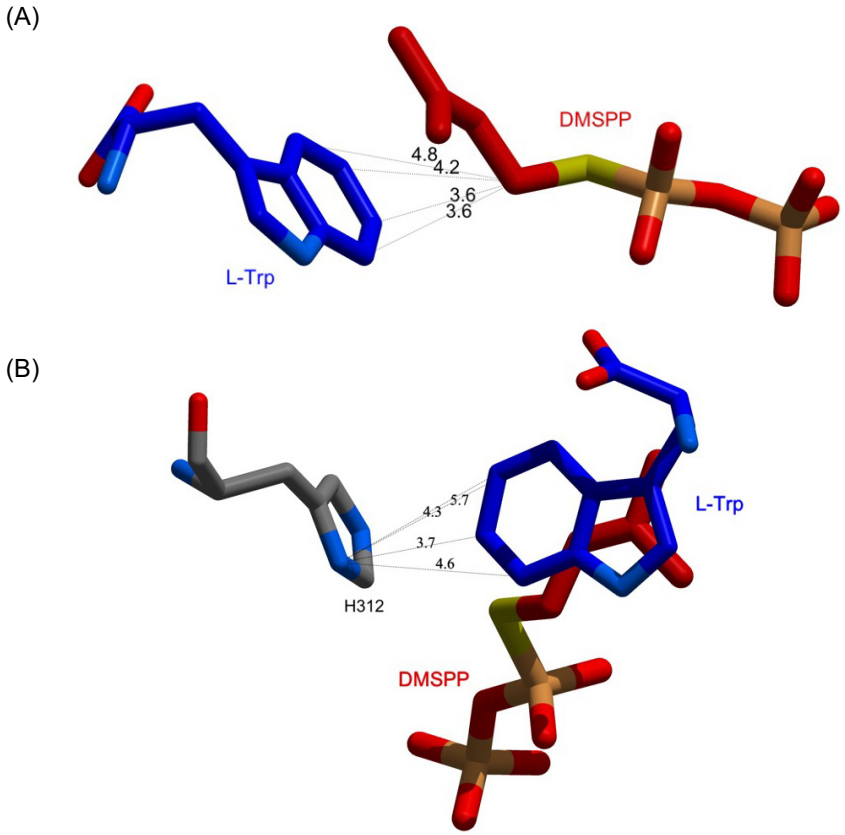

Figure S2. Close up view of the PriB active site. (A) Distance between DMAPP-analog C1' and each of the benzene carbons in tryptophan. (B) Distances between His312 basic nitrogen and each of the benzene carbons in tryptophan. Distances shown in Å.

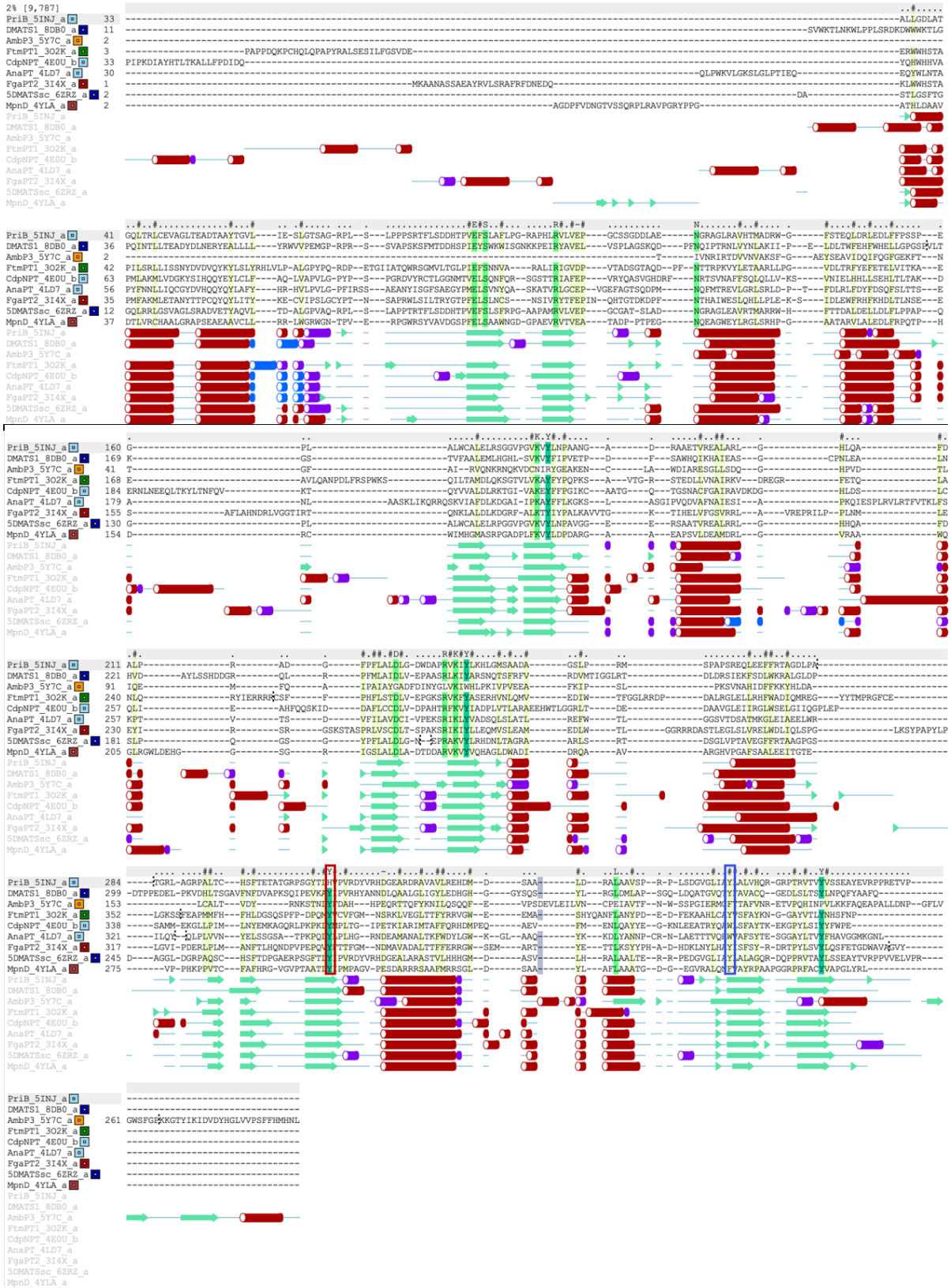

Figure S3. Structure-based alignment of PriB (PDB ID 5INJ, C6)[1] with other indole prenyltransferases; DMATS1 (PDB ID 8DB0, N1),[2] AmbP3 (PDB ID 5Y7C, C2),[3] FtmPT1 (PDB ID 3O2K, C2),[4] CdpNPT (PDB ID 4E0U, C3 rearranges to N1),[5] AnaPT (PDB ID 4LD7, C3),[6] FgaPT2 (PDB ID 3I4X, C4),[7] 5DMATSsc (PDB ID 6ZRZ, C5),[8] MpnD (PDB ID 4YLA, C7).[9] Red and blue square highlights residues that align with PriB His312 and Y364, respectively. Enzyme names and PDB ID are stated. Conserved residues are highlighted in green, pale green and yellow. Secondary structures are shown below the alignment.

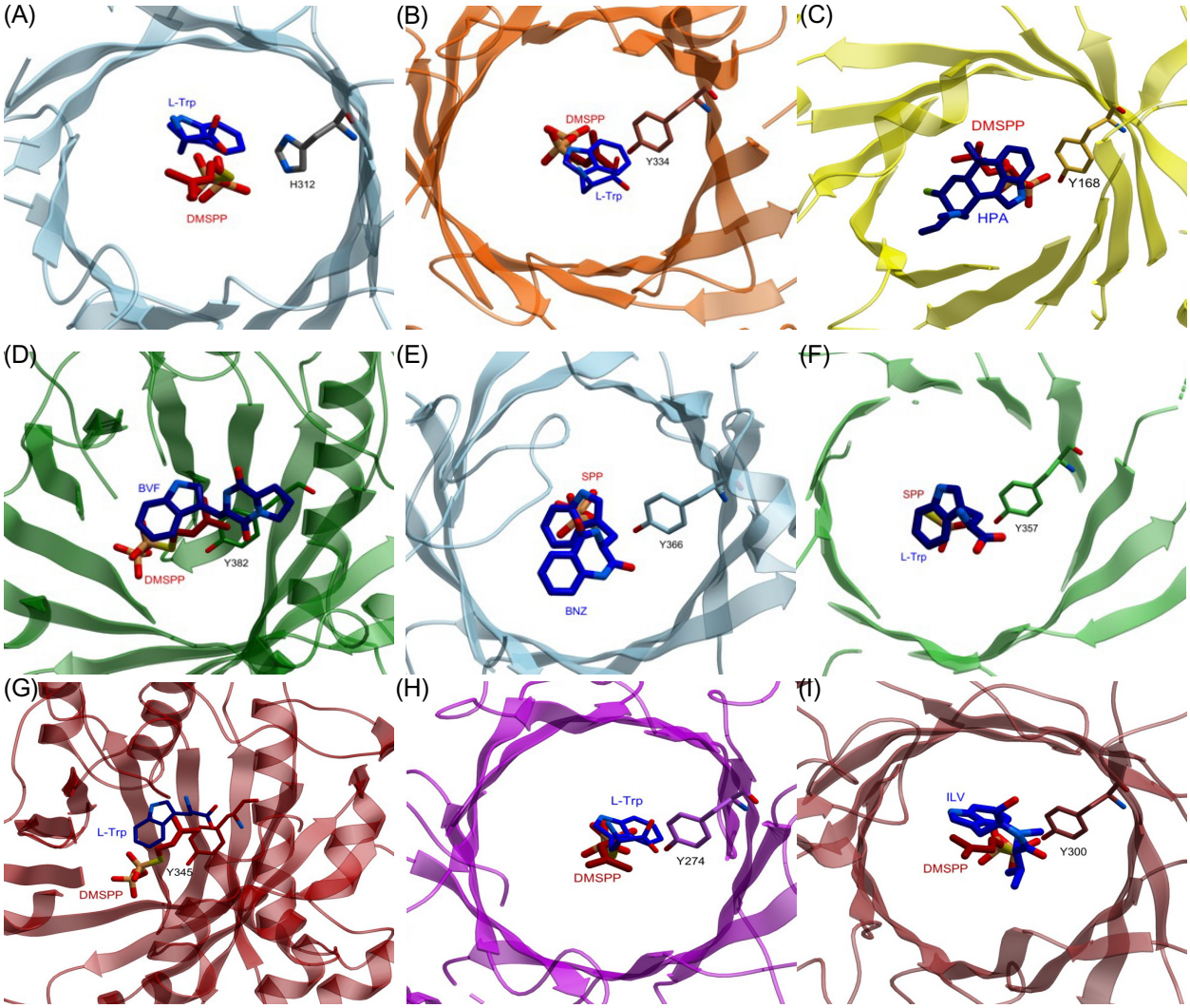

Figure S4. Close-up view of the active sites of the ligand-bound X-ray crystal structures of indole prenyltransferases showing residues that align with PriB His312. Enzymes shown are (A)PriB (PDB ID 5INJ),[1] (B) DMATS1 (PDB ID 8DB0, DMSPP added by docking),[2] (C) AmbP3 (PDB ID 5Y7C),[3] (D) FtmPT1 (PDB ID 3O2K),[4] (E) CdpNPT (PDB ID 4E0U),[5] (F) AnaPT (PDB ID 4LD7, L-Trp added by docking),[6] (G) FgaPT2 (PDB ID 3I4X),[7] (H) 5DMATSsc (PDB ID 6ZRZ),[8] (I) MpnD (PDB ID 4YLA).[9] The ligands are illustrated as ball-and-stick models with the following color code: carbon, dark blue (L-Trp) and red (DMSPP). Enzymes are shown as ribbon, His312 and aligned residues are shown as sticks. L-Trp, L-tryptophan; DMSPP, dimethylallylthiophosphate; HPA, hapalindole A; BVF, brevianamide F; SPP, thiopeptide; ILV, indolactam V.

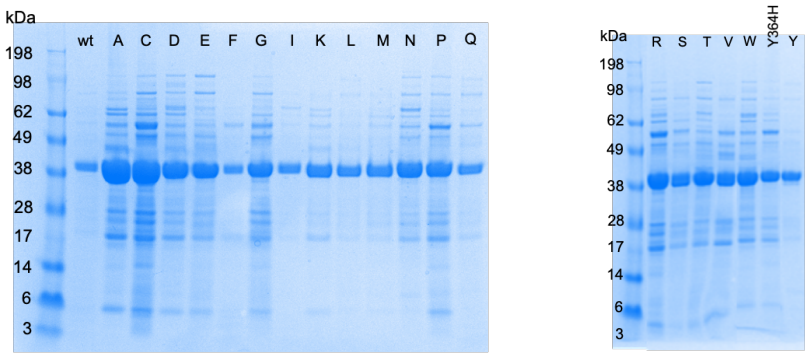

Figure S5. SDS-PAGE for *N*-His$_6$-PriB wild-type (43.3 kDa, including a 2.2 kDa His tag) and mutant enzymes characterized in this study.

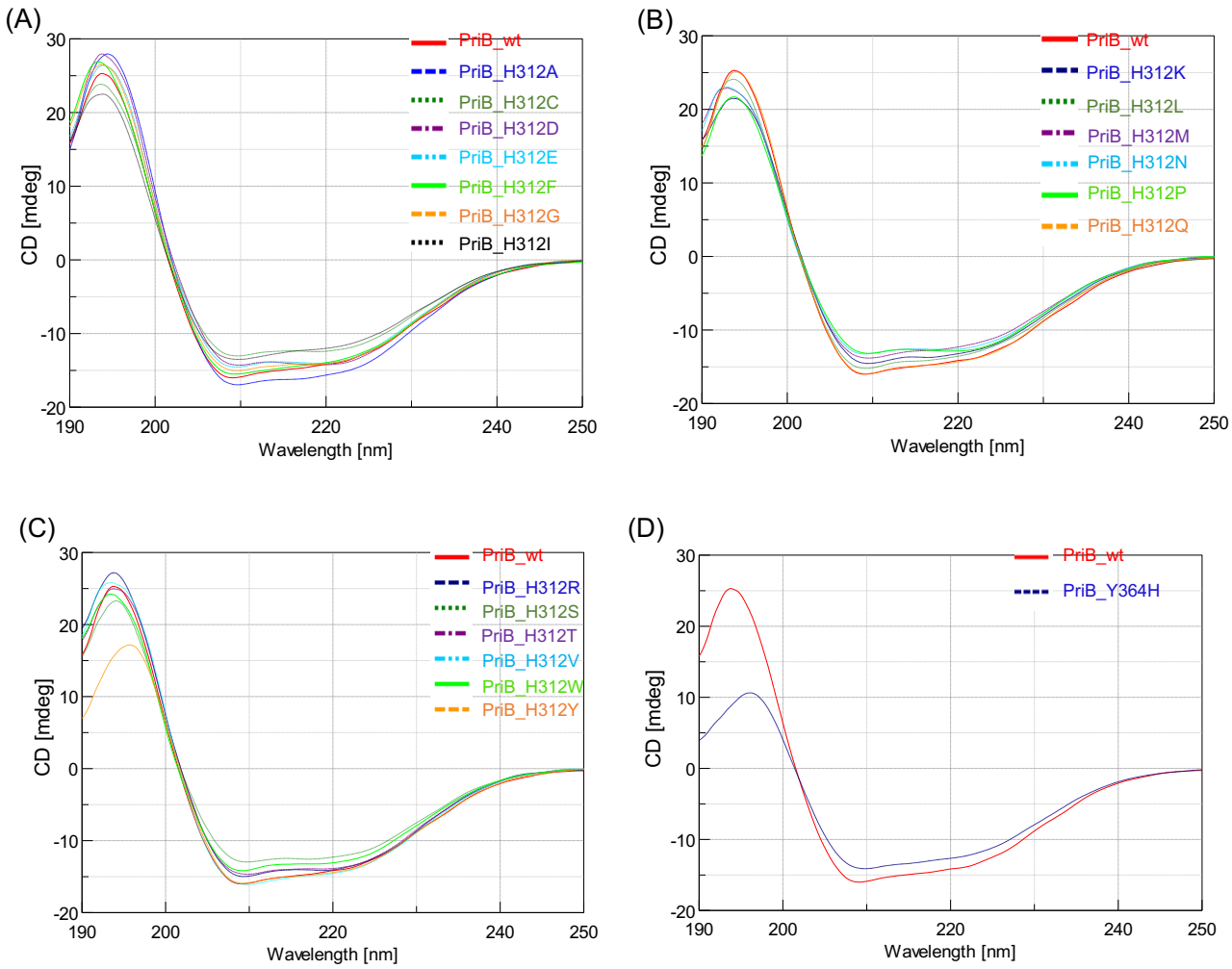

Figure S6. Circular dichroism spectra of PriB wild-type and mutant enzymes. Purified proteins were dissolved in 10 mM sodium phosphate buffer, 100 mM sodium fluoride at a concentration of approximately 200 µg ml^{-1}. Spectra were recorded on a Jasco J1500 spectropolarimeter at 25 °C using quartz cells (Alpha Nanotech) with a pathlength of 0.1 cm.

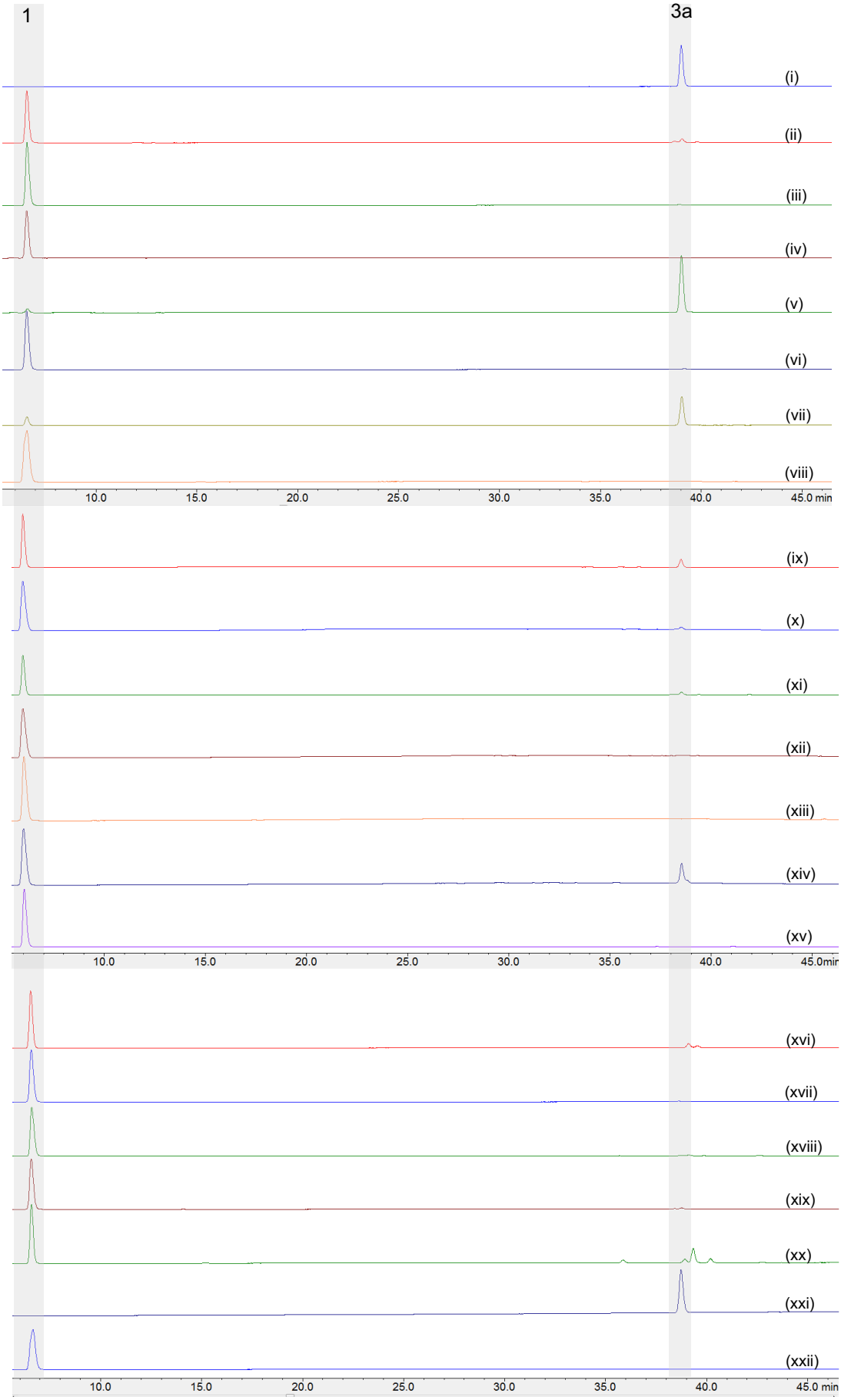
1
3a
(i)
(ii)
(iii)
(iv)
(v)
(vi)
(vii)
(viii)
10.0
15.0
20.0
25.0
30.0
35.0
40.0
45.0 min
(ix)
(x)
(xi)
(xii)
(xiii)
(xiv)
(xv)
10.0
15.0
20.0
25.0
30.0
35.0
40.0
45.0min
(xvi)
(xvii)
(xviii)
(xix)
(xx)
(xxi)
(xxii)
10.0
15.0
20.0
25.0
30.0
35.0
40.0
45.0 min

Figure S7. HPLC traces of wild-type and mutant PriB enzymatic reactions containing Tris 50 mM (pH 8.0) in 0.5 mM L-Trp (**1**) and 1 mM DMAPP (**2**) in the presence of 8.3 μM wild-type PriB (i), PriB_H312A (ii), PriB_H312C (iii), PriB_H312D (iv), PriB_H312E (v), PriB_H312F (vi), PriB_H312G (vii), PriB_H312I (viii), PriB_H312K (ix), PriB_H312L (x), PriB_H312M (xi), PriB_H312N (xii), PriB_H312P (xiii), PriB_H312Q (xiv), PriB_H312R (xv), PriB_H312S (xvi), PriB_H312T (xvii), PriB_H312V (xviii), PriB_H312W (xix), PriB_H312Y (xx), PriB_Y364H (xxi) and no enzyme (xxii). Reactions were incubated at 37 °C for 16 h and quenched with 1× methanol and monitored at A_{280}. **1**, **3a** indicate L-Trp and 6-dimethylallyltryptophan, respectively.

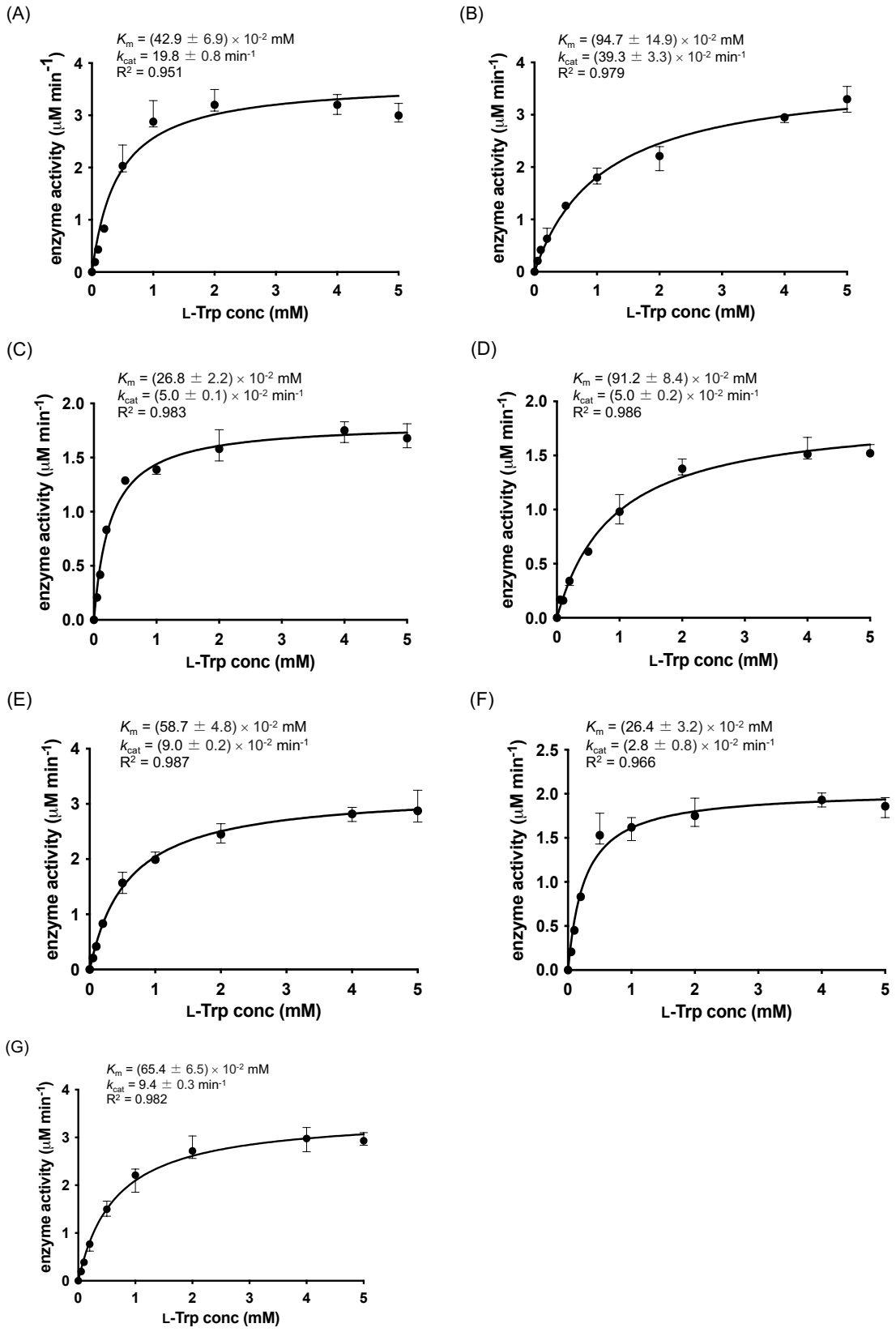

Figure S8. Steady state kinetics of recombinant wild-type and selected PriB mutants; (A) 185 × 10^{-3} μM wild-type PriB, (B) 9.2 μM PriB_H312E, (C) 36.9 μM PriB_H312G, (D) 36.9 μM PriB_H312K, (E) 36.9 μM PriB_H312Q, (F) 73.8 μM PriB_H312Y, (G) 369 × 10^{-3} μM PriB_Y364H. Assays consisted of 50 mM Tris (pH 8.0), almost saturating DMAPP (2 mM) with variable L-Trp (5 × 10^{-2} – 5 mM). Reactions were incubated at 37 °C for 240 min.

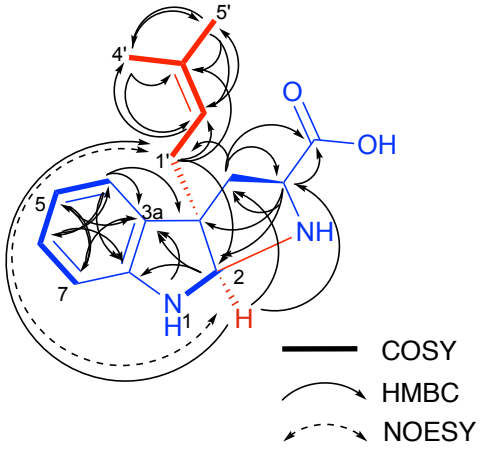

Figure S9. ^{1}H–^{1}H COSY (▬), ^{1}H–^{13}C HMBC (⌒) ^{1}H–^{1}H NOSEY (⌒) correlations of (2*S*)-3a-(3-methylbut-2-en-1-yl)-1,2,3,3a,8,8a-hexahydropyrrolo[2,3-b]indole-2-carboxylic acid (*d*$_6$–DMSO) **3b**.

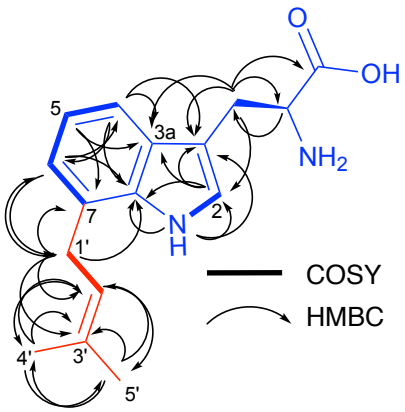

Figure S10. ^{1}H–^{1}H COSY (▬) and ^{1}H–^{13}C HMBC (⌒) correlations of (*S*)-2-amino-3-(7-(3-methylbut-2-en-1-yl)-1*H*-indol-3-yl)propanoic acid (*d*$_6$–DMSO) **3c.**

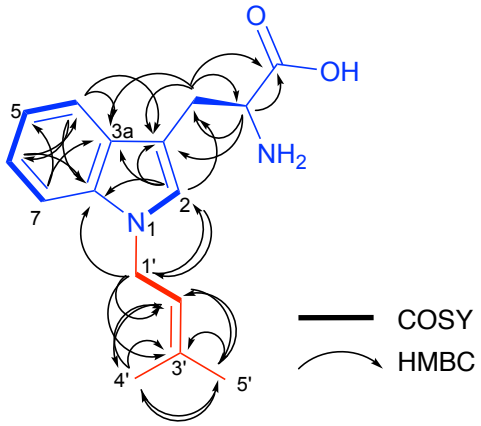

Figure S11. ^{1}H–^{1}H COSY (▬) and ^{1}H–^{13}C HMBC (⌒) correlations of 1-(3-methylbut-2-en-1-yl)-L-tryptophan (*d*$_6$–DMSO) **3d**.

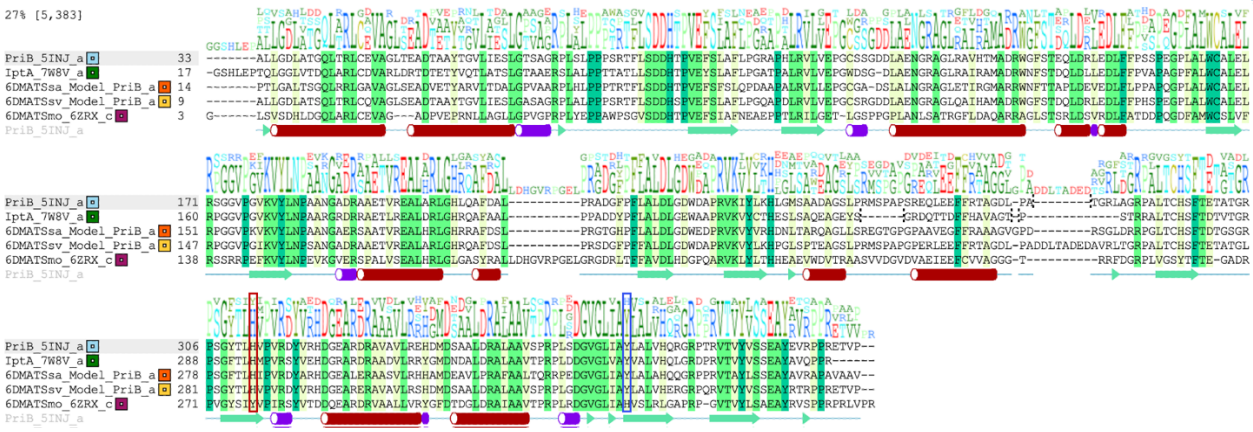

Figure S12. Structure-based alignment of PriB[1] (PDB ID 5INJ) with other C6 indole prenyltransferases; IptA[10] (PDB ID 7W8V), 6DMATSsa[11] (homology model to PriB), 6DMATSsv[11] (homology model to PriB) and 6DMATSmo[8] (PDB ID 6ZRX). Red and blue square highlights residues that align with PriB His312 and Y364, respectively. Enzyme names and PDB ID are stated. Conserved residues are highlighted in green, pale green and yellow. PriB secondary structure is shown below the alignment.

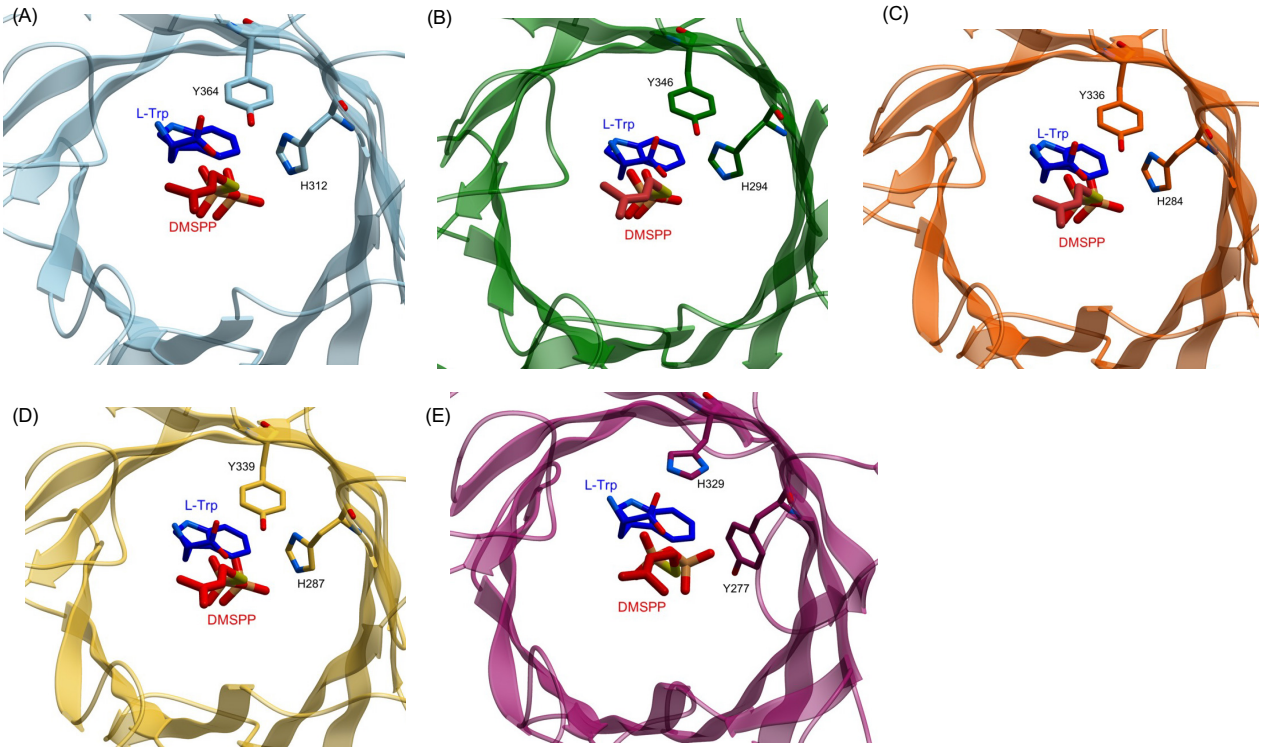

Figure S13. Close-up view of the active site of the ligand-bound structures of C6 indole prenyltransferases showing residues that align with PriB His312 and Tyr364. Enzymes shown are (A) PriB[1] (PDB ID 5INJ), (B) IptA[10] (PDB ID 7W8V), (C) 6DMATSsa[11] (homology model to PriB, docked with, (D) 6DMATSsv[11] (homology model to PriB) and (E) 6DMATSmo[8] (PDB ID 6ZRX). The ligands are illustrated as ball-and-stick models in dark blue (L-Trp) and red (DMSPP). Enzymes are shown as ribbon, His312/Tyr364 and aligned residues are shown as sticks. L-Trp, L-tryptophan; DMSPP, dimethylallylthiophosphate.

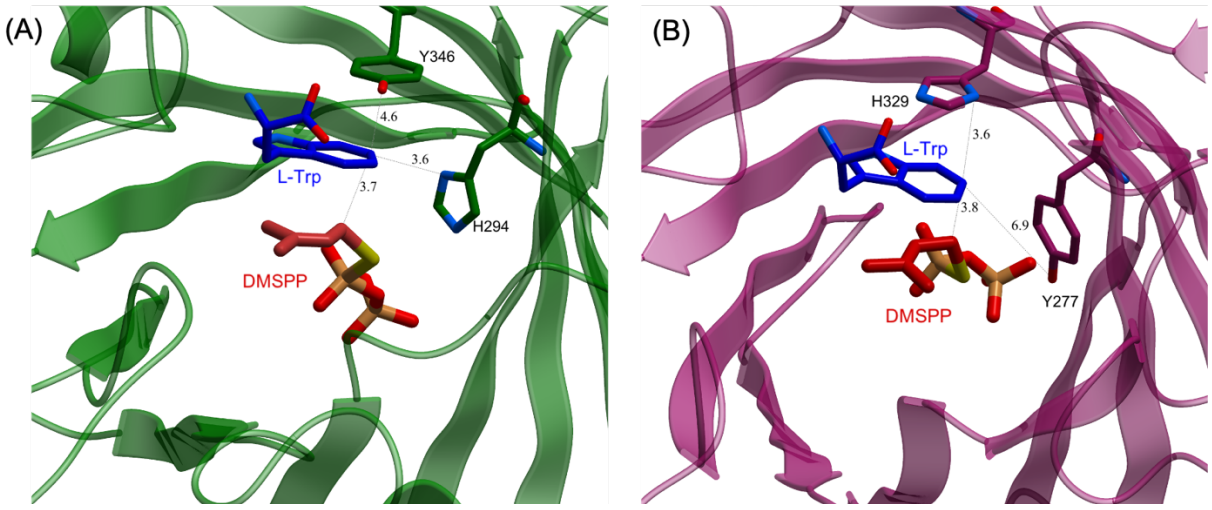

Figure S14. Close up view of (A) Ipt[10] and (B) 6DMATSmo[8] showing key distances. The ligands are illustrated as ball-and-stick models in dark blue (L-Trp) and red (DMSPP). Enzymes are shown as ribbon, His294/Tyr346 (A) and Tyr377/His329 are shown as sticks. L-Trp, L-tryptophan; DMSPP, dimethylallylthiophosphate. Distances shown in Å.

5′-
ATGGTCACAGGGGGCCGTAGCCCCATGTGCGATACCGTCGGCAGTTCATTGGCACGTCTGGAACCCACTCAAC
TTGGGGGTTTGGTGACAGACCAACTGGCTCGTCTTTGTGATGTTGCAAGACTGGACCGTACCGACACAGAGAC
CTATGTGCAGACACTGGCAACATCGTTAGGTACTGCAGCAGAGAGATCGCTTGCTTTGCCGCCGACGACGGCA
ACCCTGCTGAGCGACGACCACACACCTGTAGAATACTCGTTAGCATTCTTGCCAGGTGCTACACCGGCTCTTC
GGGTTTTAGTTGAGCCAGGTTGGGATAGCGGTGACTTGGCAGAAAATGGCCGCGCGGGCCTTCGTGCTATTCG
GGCAATGGCCGACCGTTGGAACTTTTCAACAGATCAATTGGACCTTTTGGAGGATTTGTTTTTTCCCGTCGCA
CCAGCGGGTCCTTTCGCACTTTGGTGTGCCCTTGAACTTCGCCCTGGCGGCGTGCCAGGAGTTAAGGTCTACC
TGAACCCCGCGGCACGTGGCCGTGACCGCCGCGCCGAAACTTTGCGCGAGGCATTAGATCGTTTAGGTCATCG
TCAGGCTTTCGCCGCACTGCCCCCGGCGGATGACTATCCGTTTCTGGCTTTAGACTTAGGGGAGTGGGCGGCG
CCGCGTGTAAAAGTTTATTGCACACATGAATCCCTGTCAGCTCAAGAAGCGGGCGAGTATTCGAGACTTGCAG
CCGCCGACGGGAGAGACCAGACCACAGATTTTTTTCATGCCGTAGCAGGAACTGATGCTGGCGGGACTGGCCA
ACCGTCTACTCGCCGTGCTTTAACATGCCATAGTTTCACTGACACTGTTACTGGGCGTCCCAGTGGTTTTACA
CTTCACATGCCCGTACGGTCTTACGTGGAGCACGATGGAAGAGCACGCGACCGGGCAGCAGATGTCTTGAGAC
GCTACGGGATGGATAACGATGCTCTGGATAGAGCCTTAGCGGCGGTGACGCCACGCCCCTTGGATGACGGAGT
AGGACTGGTTGCTTACGTAGCTTTGGTGCATCAGTTGGGTCGGGACCCAAGAGTGACAGTATACGTTAGCTCG
GAGGCATACGCAGTTCAGCCCCCCCGTACAGCGTTAGCCACTGGGCCGGGGATCGGTCGTTAA-3′

Figure S15. Nucleotide sequence of the codon optimized synthesized gene coding for IptA.

5′-
ATGACAACCGTACGTACAGGGGCTGAACCGGGTGGCGCACCAACTTTGGGCGCCTTAACATCAGGACAGTTGC
GCCGTTTAGGTGCTGTTGCGGGCTTAAGTGAAGCAGACGTAGAAACCTATGCGCGCGTCCTTACCGATGCACT
GGGTCCCGTTGCGGCTCGCCCTTTACATCTGCCACCACCGACCCGTACGTTTCTCAGTGACGATCATACGCCG
GTAGAATTCTCATTCTCTTTACAACCTGATGCAGCTCCAGCACTTCGTGTGCTGCTGGAGCCAGGATGTGGTG
CTGATTCCTTGGCATTAAATGGTCGCGCTGGCTTAGAGACAATTCGTGGCATGGCACGTCGTTGGAATTTCAC
TACAGCACCTTTAGATGAGGTTGAGGATTTATTTCTGCCACCTGCCCCACAAGGTCCATTGGCGTTGTGGTGT
GCGCTCGAATTACGTCCAGGTGGTGTTCCTAAAGTCAAAGTTTACCTCAATCCAGCAGCTAATGGAGCAGAAC
GCTCGGCTGCAACCGTACGTGAAGCGCTCCATCGTTTAGGACATCGTCGTGCGTTTGATTCTCTTCCTCGTGG
TACCGGCCATCCGTTCCTTGCATTGGATCTGGGTGACTGGGAAGATCCTCGTGTGAAAGTCTACGTGCGTCAT
GACAATCTCACCGCTCGTCAAGCGGGGCTTCTGAGCCGTGAGGGAACAGGTCCTGGTCCTGCAGCAGTGGAAG
GCTTCTTTCGTGCCGCAGCTGGCGTCGGTCCAGATCGTTCAGGTCTTGATCGTCGTCCTGGATTAACATGTCA
TTCATTTACGGATACGGGCAGTGGTCGTCCGAGCGGCTTTACCTTGCATATTCCGGTTCGTGATTATGCACGT
CATGATGGCGAGGCCTTGGAACGTGCGGCTAGTGTTCTTCGTCACCATGCGATGGATGAAGCAGTTCTGCCTC
GCGCTTTTGCTGCATTAACTCAACGTCGCCCCGAGGATGGCGTTGGCTTGATTGCATATCTGGCACTGGCACA
TCAACAAGGTCGTCCACCTCGTGTGACCGCATATTTGAGCTCCGAGGCGTATGCGGTCCGCGCCCCAGCCGTA
GCGGCGGTTCGTCGTCCTGTAGCAGTCCGTTGA-3′

Figure S16. Nucleotide sequence of the codon optimized synthesized gene coding for 6DMATSsa.

5′-
ATGAACGGATTCCATTCAGGCGAAGCCTTACTTGGAGACTTAGCAACCTCGCAATTAACCCGTTTATGCCAGG
TCGCAGGGTTGTCTGAGGCTGATACCGCAGCCTATACTGGCGTACTGATCGAATCCCTGGGAGCCAGCGCAGG
GCGTCCCTTGGCTTTGCCCCCACCCTCACGTACGTTTCTTTCTGACGACCATAGTCCAGTTGAGTTCAGTTTG
GCCTTCCTGCCAGGACAAGCACCGGACTTGCGTGTACTGGTGGAACCGGGATGCTCTCGTGGGGACGACTTGG
CTGAGAATGGGCGGGCAGGTCTTCAGGCAATCCATGCTATGGCCGACCGTTGGGGATTCAGCACGGATCAATT
AGATCGCCTGGAAGACTTGTTCTTCCCGCACTCGCCTGAAGGCCCACTTGCGCTTTGGTGCGCTCTGGAGTTA
CGGCCGGGTGGTGTTCCCGGGATTAAAGTCTATCTTAATCCTAGTGCAAATGGCGCTGATCGCGCCGCTGAAA
CCGTTCGCGAAGCCCTGGCGCGCCTTGGGCACCGGCAAGCGTTCGATTCCCTTCCCCGGTCAGACGGATTTCC
CTTCTTCGCCTTAGACTTGGGTGATTGGGATGCTCCACGGGTAAAAGTTTACCTGAAACACCCGGGCCTTTCA
CCTACAGAGGCCGGTAGCCTGCCACGTATGTCACCTGCACCCGGGCCCGAGCGCCTGGAAGAGTTCTTTCGGA
CGGCGGGAGACTTACCCGCTGACGATTTGACGGCAGATGAGGATGCGGTACGCCTTACAGGCAGACCCGCTCT
GACCTGCCACAGCTTTACAGAGACAGCAACTGGCCTTCCTTCTGGTTATACGCTGCATGTTCCCGTAAGAGAT
TACGTCCGGCATGACGGTGAGGCGCGGGAGCGTGCTGTTGCCGTTTTACGTTCGCATGACATGGACTCAGCAG
CCTTGGATCGGGCTTTGGCCGCCGTTTCCCCTCGCCCCTTAGGAGACGGAGTAGGGCTTATTGCCTATCTTGC
TCTTGTACACGAGAGAGGCAGACCGCAACGTGTTACTGTGTACGTCTCATCCGAGGCCTATAGAACTCGGCCT
CCGCGCGAGACCGTACCGACGCGCGACCGGGTGCGTGCCGGGCTGTAA-3′

Figure S17. Nucleotide sequence of the codon optimized synthesized gene coding for 6DMATSsv.

5′-
ATGGCGGGTCTGTCTGTTTCTGACCACCTGGACGGTCAGCTGGCGCGTCTGTGCGAAGTTGCGGGTGCGGACC
CGGTTGAACCGCGTAACCTGCTGGCGGGTCTGCTGGGTCCGGTTGGTCCGCGTCCGCTGTACGAACCGCCGGC
GTGGCCGTCTGGTGTTTCTGACGACCACACCCCGGTTGAATTCTCTATCGCGTTCAACGAAGCGGAACCGCCG
ACCCTGCGTATCCTGGGTGAAACCCTGGGTTCTCCGCCGGGTCCGCTGGCGAACCTGTCTGCGACCCGTGGTT
TCCTGGACGCGCAGGCGCGTCGTGCGGGTCTGTCTACCTCTCGTCTGGACTCTGTTCGTGACCTGTTCGCGAC
CGACGACCCGCAGGGTGACTTCGCGATGTGGTGCTCTCTGGTTTTCCGTTCTTCTCGTCGTCCGGAATTCAAA
GTTTACCTGAACCCGGAAGTTAAAGGTGTTGAACGTTCTCCGGCGCTGGTTTCTGAAGCGCTGCACCGTCTGG
GTCTGGGTGCGTCTTACCGTGCGCTGCTGGACCACGGTGTTCGTCCGGGTGAACTGGGTCGTGGTGACCGTCT
GACCTTCTTCGCGGTTGACCTGCACGACGGTCCGCAGGCGCGTGTTAAACTGTACCTGACCCACCACGAAGCG
GAAGTTTGGGACGTTACCCGTGCGGCGTCTGTTGTTGACGGTGTTGACGTTGCGGAAATCGAAGAATTCTGCG
TTGTTGCGGGTGGTGGTACCCGTCGTTTCGACGGTCGTCCGCTGGTTGGTTCTTACACCTTCACCGAAGGTGC
GGACCGTCCGGTTGGTTACTCTATCTACGTTCCGATCCGTTCTTACGTTACCGACGACCAGGAAGCGCGTGAC
CGTGTTGCGGCGCTGCTGGTTCGTTACGGTTTCGACACCGACGGTCTGGACCGTGCGATCGCGGCGGTTACCC
CGCGTCCGCTGCGTGACGGTGTTGGTCTGATCGCGCACGTTTCTCTGCGTCTGGGTGCGCCGCGTCCGGGTGT
TACCGTTTACCTGTCTGCGGAAGCGTACCGTGTTTCTCCGCCGCGTCCGCGTCGTATGCCGGCGGGTCGTGAC
GTTTCTCCGGCGCCGGTTGGTCGTACCCGTCCGTAA-3′

Figure S18. Nucleotide sequence of the codon optimized synthesized gene coding for 6DMATSmo.

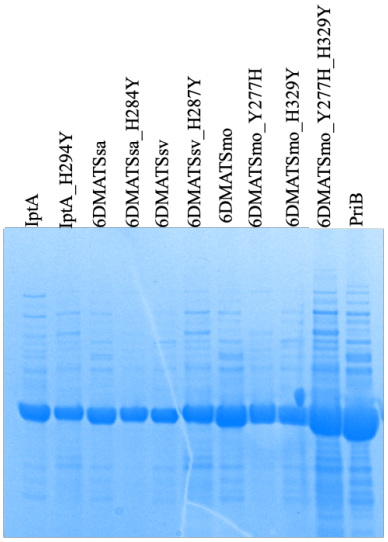

Figure S19. SDS-PAGE for *N*-His$_6$-IptA (43.5 kDa, including a 2.2 kDa His tag), *N*-His$_6$-6DMATSsa (42.1 kDa, including a 2.2 kDa His tag), *N*-His$_6$-6DMATSsv (43.0 kDa, including a 2.2 kDa His tag), *N*-His$_6$-6DMATSmo (42.8 kDa, including a 2.2 kDa His tag) wild-type and mutant enzymes characterized in this study.

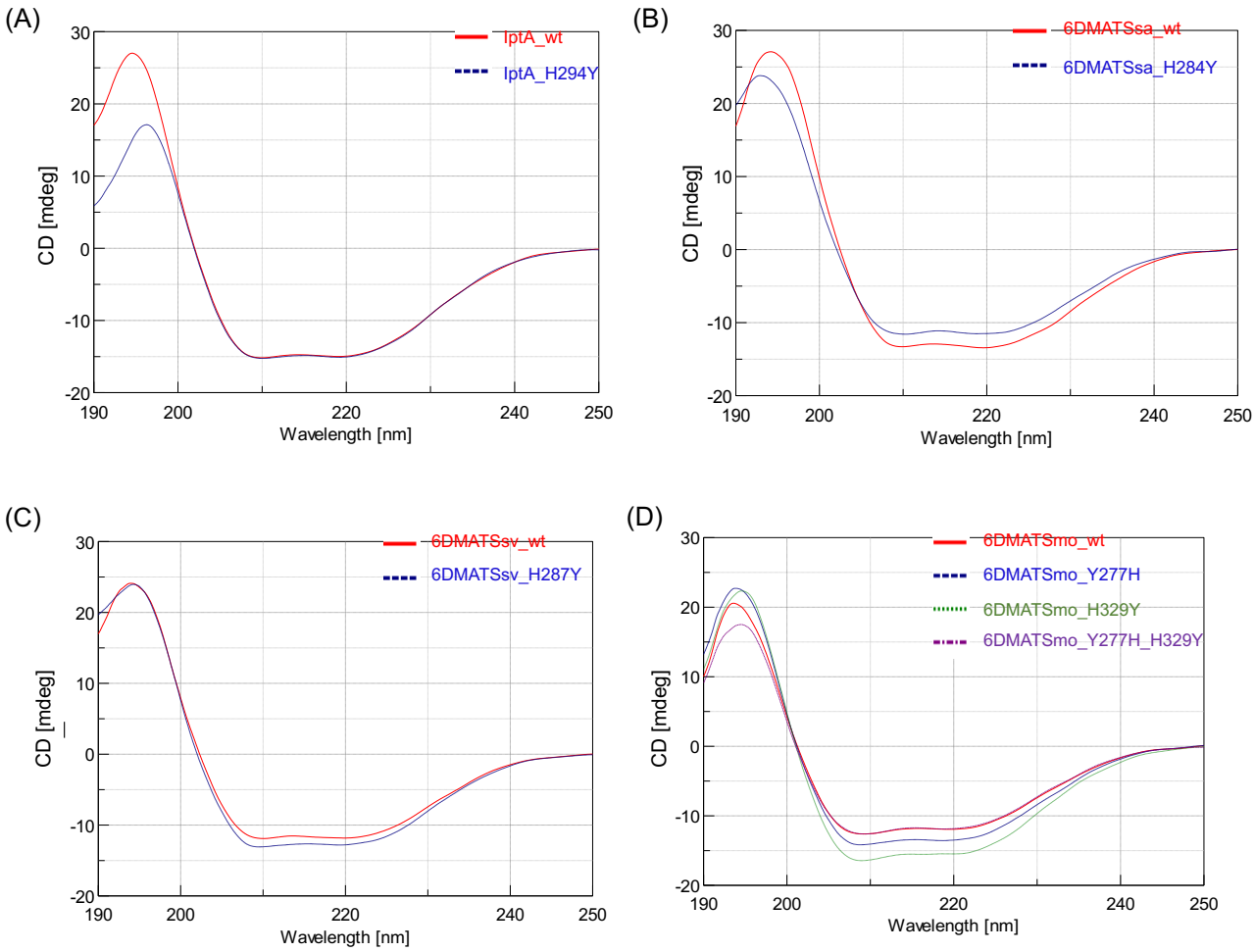

Figure S20. Circular dichroism spectra of (A) IptA, (B) 6DMATSsa, (C) 6DMATSsv and (D) 6DMATSmo wild-type and mutant enzymes. Purified proteins were dissolved in 10 mM sodium phosphate buffer, 100 mM sodium fluoride at a concentration of approximately 200 µg ml^{-1}. Spectra were recorded on a Jasco J1500 spectropolarimeter at 25 °C using quartz cells (Alpha Nanotech) with a pathlength of 0.1 cm.

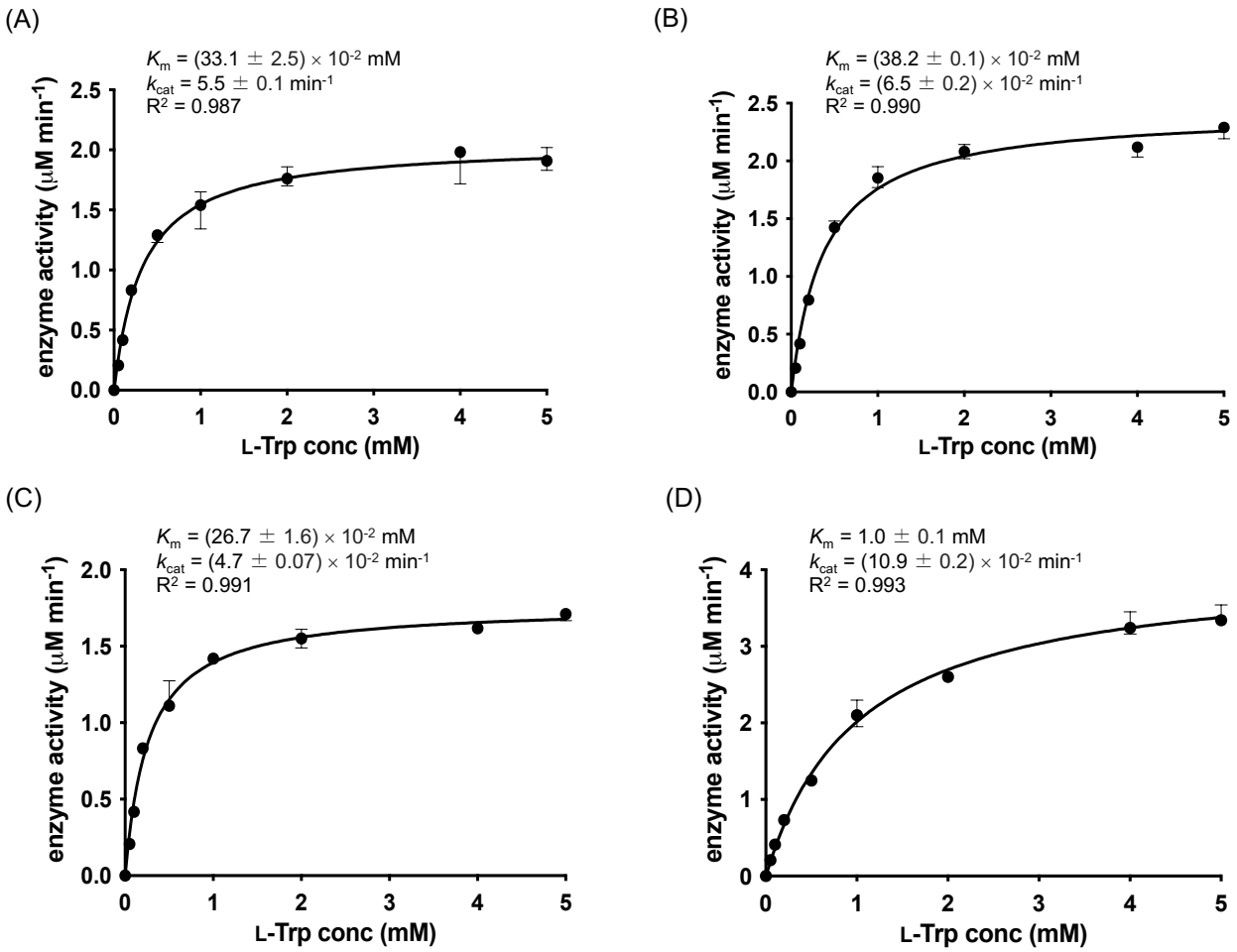

Figure S21. Steady state kinetics of recombinant (A) 374 × 10^{-3} μM 6DMATSmo wild-type and mutants (B) 37.4 μM 6DMATSmo_Y277H, (C) 37.4 μM 6DMATSmo_H329Y, (D) 37.4 μM 6DMATSmo_Y277H_H329Y. Assays consisted of 50 mM Tris (pH 8.0), almost saturating DMAPP (2 mM) with variable L-Trp (5 × 10^{-2} – 5 mM). Reactions were incubated at 37 °C for 240 min.

Figure S22. Sequence alignment of PriB with AtmD,[12] JanD[13] and PaxD.[14] Red boxes highlight amino acid residues that align with PriB His312 and Tyr364.

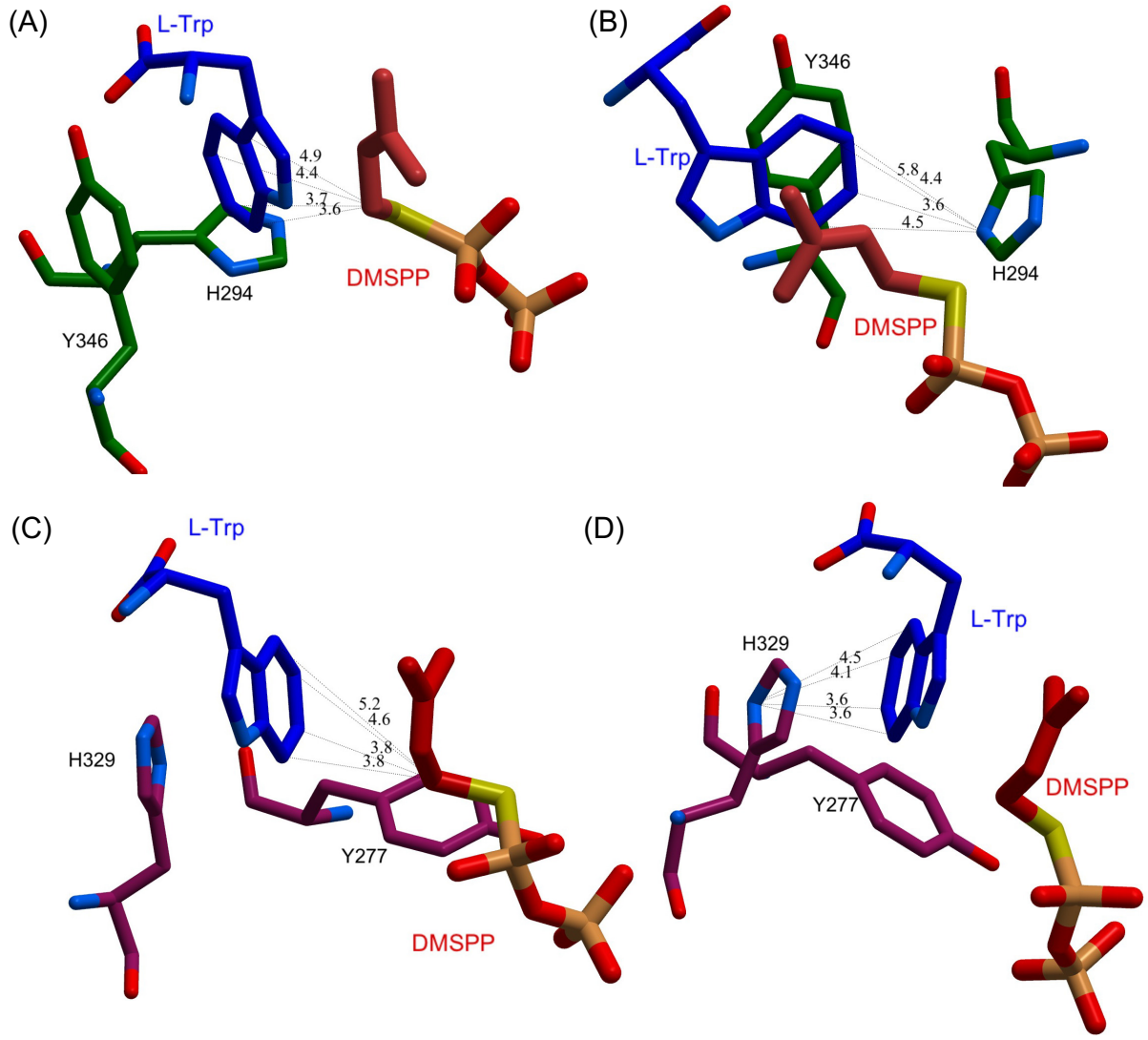

Figure S23. Close up view of IptA[10] (A and B) and 6DMATSmo[8] (C and D) showing key distances. The ligands are illustrated as ball-and-stick models in dark blue (L-Trp) and red (DMSPP). His294/Tyr346 (A and B) and Tyr377/His329 (C and D) are shown as sticks. L-Trp, L-tryptophan; DMSPP, dimethylallylthiophosphate. Distances shown in Å.

III-Supporting Tables

Table S1. Primer names and sequences used in this study. Underlined nucleotide residues are sites of mutations.

Primer Name	Primer Sequence
PriB_H312A-F	5′–CTA CAC CCT CGC TGT GCC GGT CCG CGA CTA CGT CCG G–3′
PriB_H312C-F	5′–CTA CAC CCT CTG TGT GCC GGT CCG CGA CTA CGT CCG G–3′
PriB_H312D-F	5′–CTA CAC CCT CGA TGT GCC GGT CCG CGA CTA C–3′
PriB_H312E-F	5′–CTA CAC CCT CGA AGT GCC GGT CCG CGA CTA CG–3′
PriB_H312F-F	5′–CTA CAC CCT CTT TGT GCC GGT CCG CGA CTA CGT CCG G–3′
PriB_H312G-F	5′–CTA CAC CCT CGG TGT GCC GGT CCG CGA CTA CGT CCG G–3′
PriB_H312I-F	5′–CTA CAC CCT CAT TGT GCC GGT CCG CGA CTA CGT CCG G–3′
PriB_H312K-F	5′–CTA CAC CCT CAA AGT GCC GGT CCG CGA CTA C–3′
PriB_H312L-F	5′–CTA CAC CCT CTT AGT GCC GGT CCG CGA CTA CGT CCG G–3′
PriB_H312M-F	5′–CTA CAC CCT CAT GGT GCC GGT CCG CGA CTA CGT CCG GCA CGA CGG–3′
PriB_H312N-F	5′–CTA CAC CCT CAA TGT GCC GGT CCG CGA CTA C–3′
PriB_H312P-F	5′–CTA CAC CCT CCC TGT GCC GGT CCG CGA CTA CGT CC–3′
PriB_H312Q-F	5′–CTA CAC CCT CCA AGT GCC GGT CCG CG–3′
PriB_H312R-F	5′–CTA CAC CCT CAG AGT GCC GGT CCG CGA CTA CGT CCG–3′
PriB_H312S-F	5′–CTA CAC CCT CTC AGT GCC GGT CCG CGA CTA CGT CCG GCA C–3′
PriB_H312T-F	5′–CTA CAC CCT CAC TGT GCC GGT CCG CGA CTA CGT CCG GCA C–3′
PriB_H312V-F	5′–CTA CAC CCT CGT AGT GCC GGT CCG CGA CTA CGT CCG GCA CG–3′
PriB_H312W-F	5′–CTA CAC CCT CTG GGT GCC GGT CCG CGA CTA CGT CCG G–3′
PriB_H312Y-F	5′–CTA CAC CCT CTA TGT GCC GGT CCG CGA C–3′
PriB_H312X-R	5′–CCG CTG GGC CGC CCG GTC–3′
PriB_Y364H-F	5′–CCT GAT CGC CCA TCT GGC ACT–3′
PriB_Y364H-R	5′–CCC ACC CCG TCA CTC AGC–3′
IptA_H294Y-F	5′–TTT TAC ACT TTA TAT GCC CGT ACG GTC TTA C–3′
IptA_H294Y-R	5′–CCA CTG GGA CGC CCA GTA–3′
6DMATSsa_H284Y-F	5′–CTT TAC CTT GTA TAT TCC GGT TCG TGA TTA TG–3′
6DMATSsa_H284Y-R	5′–CCG CTC GGA CGA CCA CTG–3′
6DMATSsv_H287Y-F	5′–TTA TAC GCT GTA TGT TCC CGT AAG–3′
6DMATSsv_H287Y-R	5′–CCA GAA GGA AGG CCA GTT–3′
6DMATSmo_Y277H-F	5′–TTA CTC TAT CCA TGT TCC GAT CCG TTC TTA CGT TAC C–3′
6DMATSmo_Y277H-R	5′–CCA ACC GGA CGG TCC GCA–3′
6DMATSmo_H329Y-F	5′–TCT GAT CGC GTA TGT TTC TCT GCG–3’
6DMATSmo_H329Y-R	5′–CCA ACA CCG TCA CGC AGC–3′
T7	5′–TAA TAC GAC TCA CTA TAG GG–3′
T7 Terminator	5′–GCT AGT TAT TGC TCA GCG G–3′

Table S2. Summary of molecular formula, calculated and observed high-resolution mass spectrometry data of prenylated tryptophans generated in study.

Compound	Molecular Formula	Ionization	Calculated Mass (*m/z*)	Observed Mass (*m/z*)
3b	$C_{16}H_{21}N_2O_2$	$[M + H]^+$	273.1598	273.1589
3c	$C_{16}H_{21}N_2O_2$	$[M + H]^+$	273.1598	273.1589
3d	$C_{16}H_{21}N_2O_2$	$[M + H]^+$	273.1598	273.1591

Table S3. ^1H (400 MHz) and ^{13}C (100 MHz) NMR spectroscopic data of (2*S*)-3a-(3-methylbut-2-en-1-yl)-1,2,3,3a,8,8a-hexahydropyrrolo[2,3-b]indole-2-carboxylic acid **3b** (d_6–DMSO).

Residue	Position	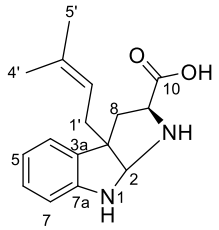 **(C3) 3b**[a]	
		δ_C, type	**δ_H, mult (*J* in Hz)**
L-Trp			
	1		6.34, s
	2	82.3, CH	4.76, s
	3	56.9, C	
	3a	133.2, C	
	4	123.2, CH	6.99, d (7.3)
	5	117.7, CH	6.58, t (7.6)
	6	127.6, CH	6.93, t (7.6)
	7	124.2, CH	6.48, d (7.7)
	7a	148.8, C	
	8	40.4, CH_2	2.36 – 2.30, m
			2.21, dd (12.9, 5.6)
	9	59.2, CH	3.71, dd (8.5, 5.7)
	C=O	172.2, C	
DMA			
	1'	36.0, CH_2	2.28, m
	2'	119.7, CH	5.04, t (7.2)
	3'	133.6, C	
	4'	17.8, CH_3	1.51, s
	5'	25.7, CH_3	1.63, s

Assignments supported by 2D COSY, HSQC, HMBC experiments and by comparison with related compounds from literatures. [a]see Supporting NMR Spectral Data. DMA, dimethylallyl.

Table S4. ^{1}H (400 MHz) and ^{13}C (100 MHz) NMR spectroscopic data of (*S*)-2-amino-3-(7-(3-methylbut-2-en-1-yl)-1*H*-indol-3-yl)propanoic acid **3c** and 1-(3-methylbut-2-en-1-yl)-L-tryptophan **3d** (d_6–DMSO).

Residue	Positn	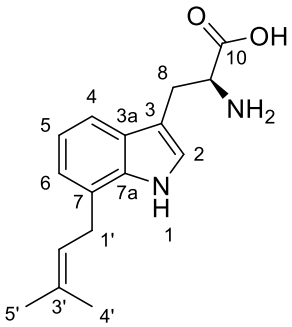 **(C7) 3c**[a]		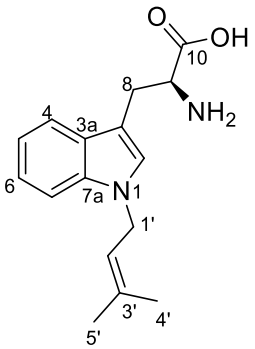 **(N1) 3d**[a]	
		δ_C, type	**δ_H, mult (*J* in Hz)**	**δ_C, type**	**δ_H, mult (*J* in Hz)**
L-Trp					
	1		10.80, s		
	2	123.9, CH	7.18, s	127.0, CH	7.17, s
	3	109.7, C		109.2, C	
	3a	127.1, C		127.7, C	
	4	116.0, CH	7.38, d (7.7)	118.7, CH	7.57, d (7.9)
	5	118.6, CH	6.91, t (7.5)	118.4, CH	7.01, t (7.4)
	6	120.0, CH	6.84, d (6.9)	121.0, CH	7.11, t (7.6)
	7	124.2, C		109.7, CH	7.35, d (8.2)
	7a	135.0, C		135.9, C	
	8	27.1, CH_2	2.93, dd (15.1, 9.1) 3.31 – 3.26, m	27.0, CH_2	2.93, dd (15.1, 8.8) 3.27, bm
	9	54.4, CH	3.51, m	54.7, CH	3.49, bm
	C=O	169.8, C		169.6, C	
DMA					
	1'	29.0, CH_2	3.51, d (7.2)	43.4, CH_2	4.69, d (6.7)
	2'	122.2, CH	5.42, t (7.3)	120.6, CH	5.32, t (6.8)
	3'	131.9, C		134.9, C	
	4'	17.7, CH_3	1.71, s	17.8, CH_3	1.81, s
	5'	25.5, CH_3	1.71, s	25.3, CH_3	1.71, s

Assignments supported by 2D COSY, HSQC, HMBC experiments and by comparison with related compounds from literatures. [a]see Supporting NMR Spectral Data. DMA, dimethylallyl.

Table S5. Residues that align with PriB His312 (position 1) and Tyr364 (position 2) present in selected indole prenyltransferases.

Enzyme	Position 1	Position 2
PriB[1]	His312	Tyr364
DMATS1[2]	Tyr334	Tyr389
AmbP3[3]	Tyr168	Tyr225
FtmPT1[4]	Tyr382	Tyr435
CdpNPT[5]	Tyr366	Trp319
AnaPT[6]	Tyr357	Trp410
FgaPT2[7]	Tyr345	Tyr398
5DMATSsc[8]	Tyr274	Tyr326
MpnD[9]	Tyr300	Phe350
IptA[10]	His294	Tyr346
6DMATSsa[11]	His284	Tyr336
6DMATSsv[11]	His287	Tyr339
6DMATSmo[8]	Tyr277	His329
AtmD[12]	Tyr346	His397
JanD[13]	Tyr350	His402
PaxD[14]	Tyr349	His401

IV-Supporting References

[1] S. I. Elshahawi, H. Cao, K. A. Shaaban, L. V. Ponomareva, T. Subramanian, M. L. Farman, H. P. Spielmann, G. N. Phillips, J. S. Thorson, S. Singh, *Nat. Chem. Biol.* **2017**, *13*, 366–368.

[2] S. A. Eaton, T. A. Ronnebaum, B. W. Roose, D. W. Christianson, *Biochemistry* **2022**, *61*, 2025–2035.

[3] C. P. Wong, T. Awakawa, Y. Nakashima, T. Mori, Q. Zhu, X. Liu, I. Abe, *Angew. Chem.* **2018**, *57*, 560–563.

[4] M. Jost, G. Zocher, S. Tarcz, M. Matuschek, X. Xie, S.-M. Li, T. Stehle, *J. Am. Chem. Soc.* **2010**, *132*, 17849–17858.

[5] J. Chen, H. Morita, R. Kato, H. Noguchi, S. Sugio, I. Abe, *Acta Crystallograph. Sect. F Struct. Biol. Cryst. Commun.* **2012**, *68*, 355–358.

[6] X. Yu, G. Zocher, X. Xie, M. Liebhold, S. Schütz, T. Stehle, S.-M. Li, *Chem. Biol.* **2013**, *20*, 1492–1501.

[7] U. Metzger, C. Schall, G. Zocher, I. Unsöld, E. Stec, S.-M. Li, L. Heide, T. Stehle, *Proc. Natl. Acad. Sci. U. S. A.* **2009**, *106*, 14309–14314.

[8] E. Ostertag, L. Zheng, K. Broger, T. Stehle, S.-M. Li, G. Zocher, *J. Mol. Biol.* **2021**, *433*, 166726.

[9] T. Mori, L. Zhang, T. Awakawa, S. Hoshino, M. Okada, H. Morita, I. Abe, *Nat. Commun.* **2016**, *7*, 10849.

[10] H. Suemune, D. Nishimura, K. Mizutani, Y. Sato, T. Hino, H. Takagi, Y. Shiozaki-Sato, S. Takahashi, S. Nagano, *Biochem. Biophys. Res. Commun.* **2022**, *593*, 144–150.

[11] J. Winkelblech, S.-M. Li, *Chembiochem* **2014**, *15*, 1030–1039.

[12] C. Liu, A. Minami, M. Noike, H. Toshima, H. Oikawa, T. Dairi, *Appl. Environ. Microbiol.* **2013**, *79*, 7298–7304.

[13] M. J. Nicholson, C. J. Eaton, C. Stärkel, B. A. Tapper, M. P. Cox, B. Scott, *Toxins* **2015**, *7*, 2701–2722.

[14] C. Liu, M. Noike, A. Minami, H. Oikawa, T. Dairi, *Appl. Microbiol. Biotechnol.* **2014**, *98*, 199–206.

V-Supporting Mass and NMR Spectra

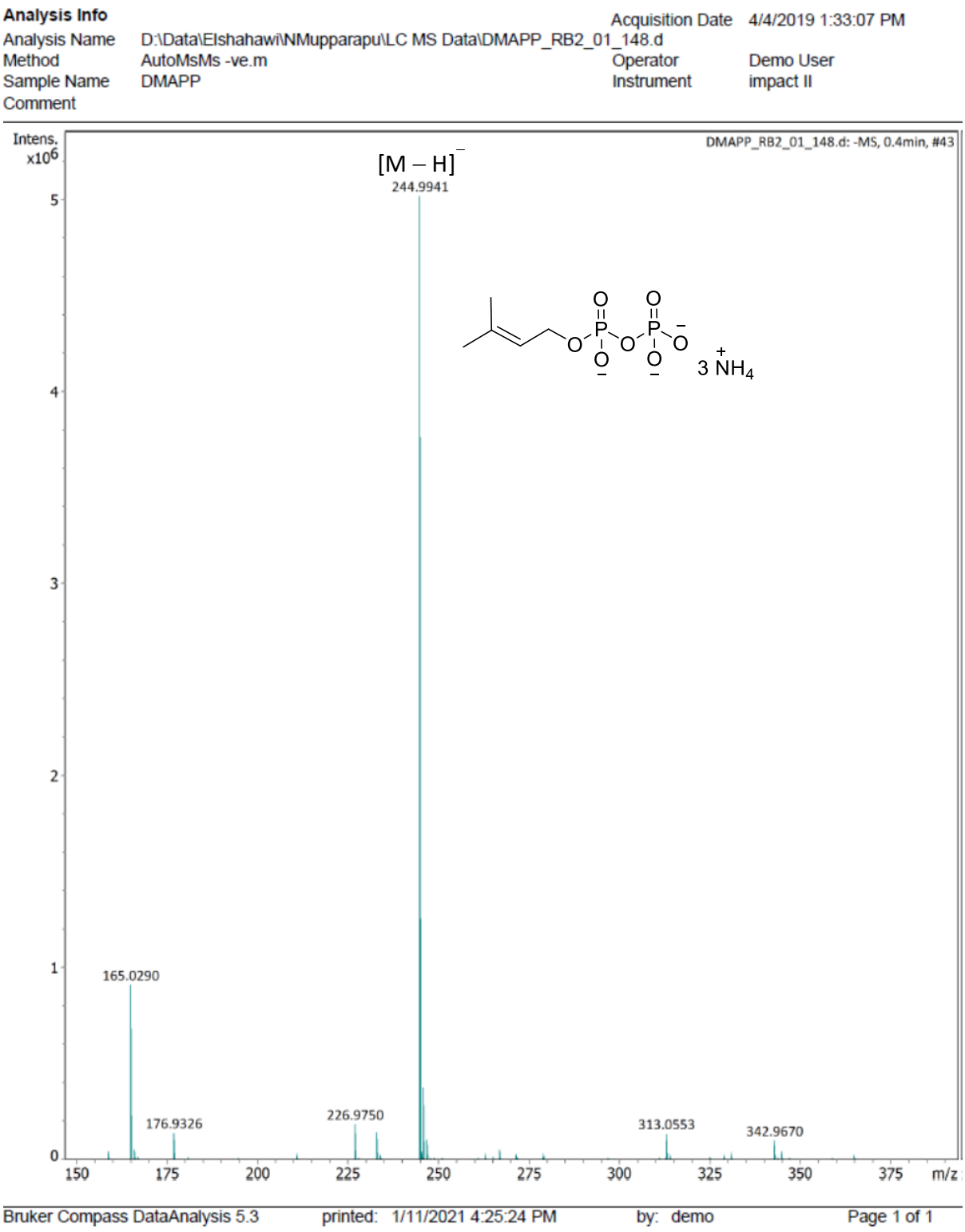

LC-HR-ESI-MS data of dimethylallyl diphosphate **2.**

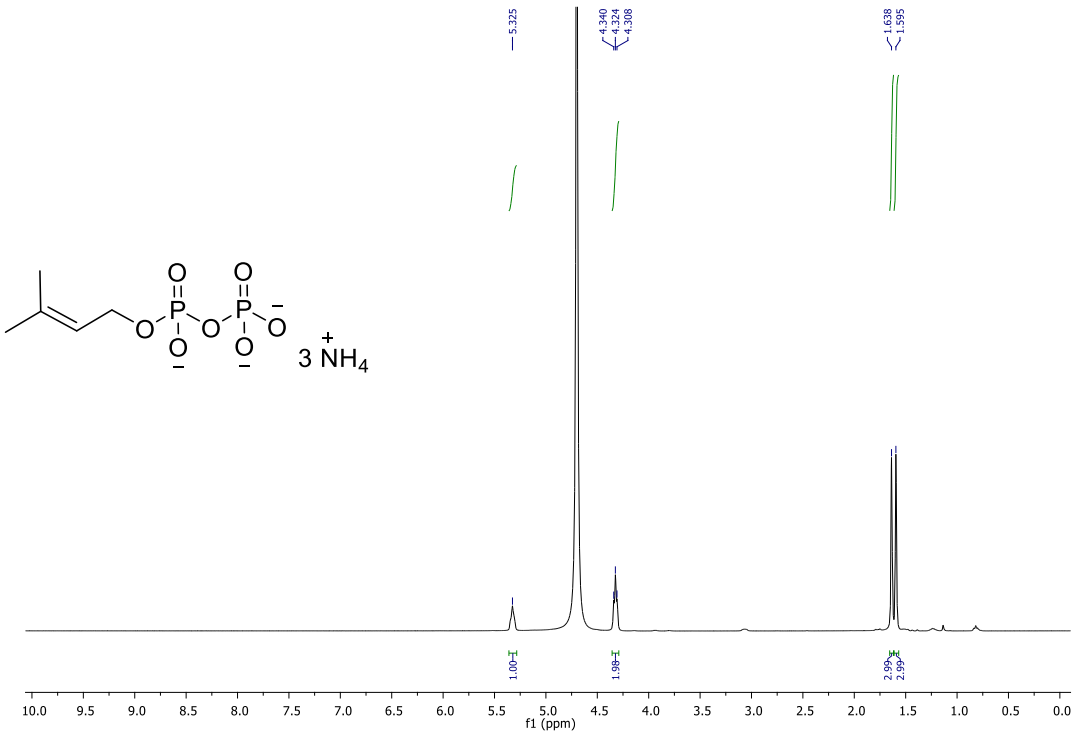

^{1}H NMR (D_2O, 400 MHz) of dimethylallyl diphosphate **2**.

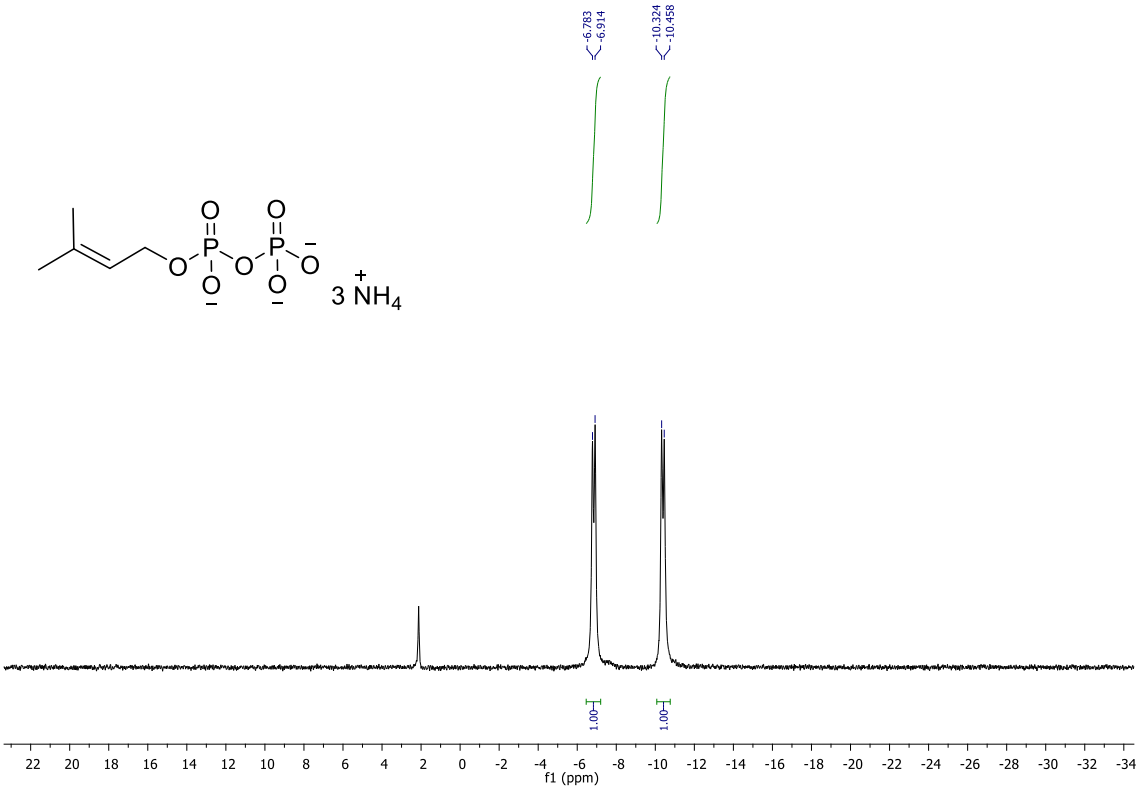

^{31}P NMR (D_2O, 164 MHz) of dimethylallyl diphosphate **2**.

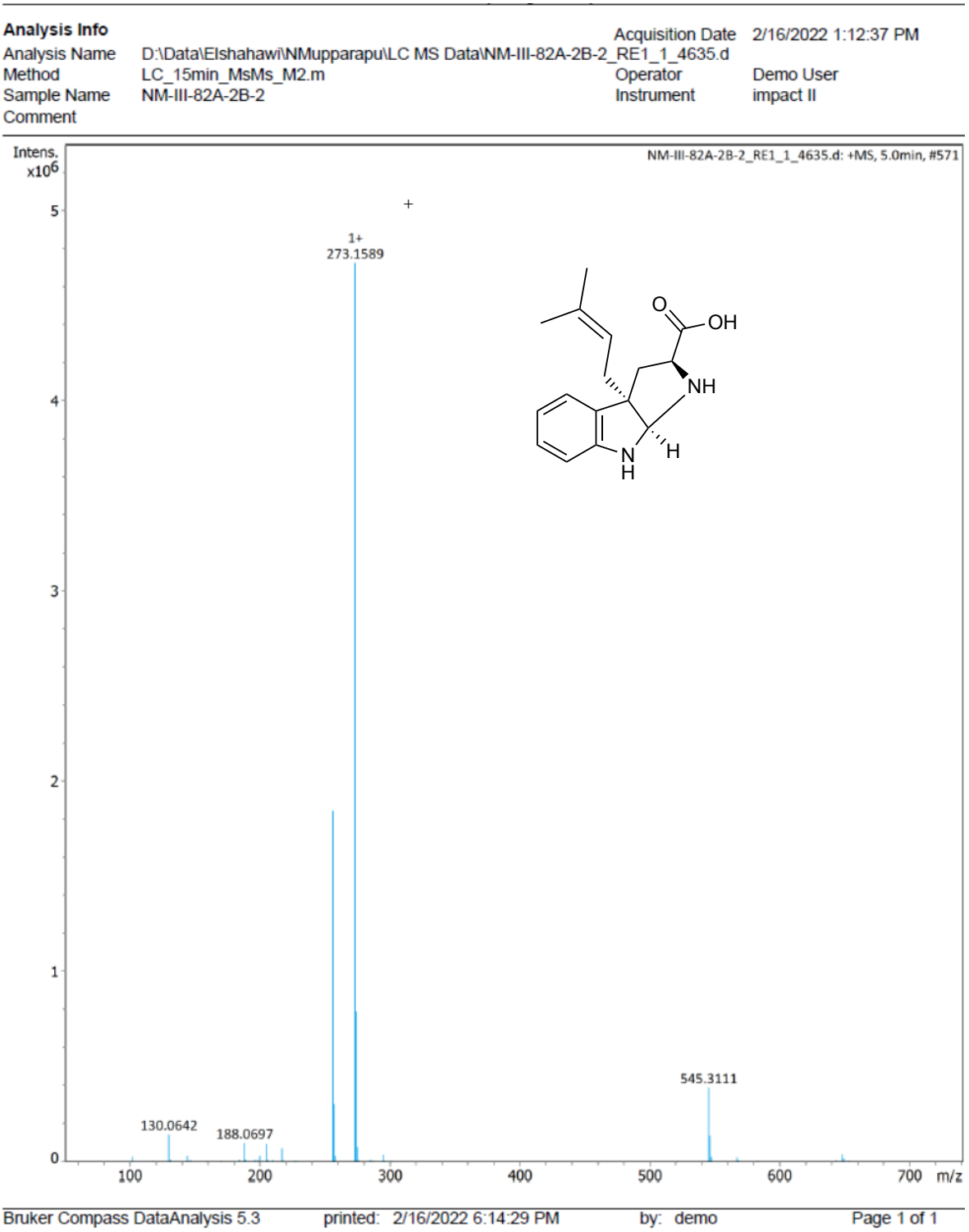

LC-HR-ESI-MS of (2*S*)-3a-(3-methylbut-2-en-1-yl)-1,2,3,3a,8,8a-hexahydropyrrolo[2,3-b]indole-2-carboxylic acid **3b**.

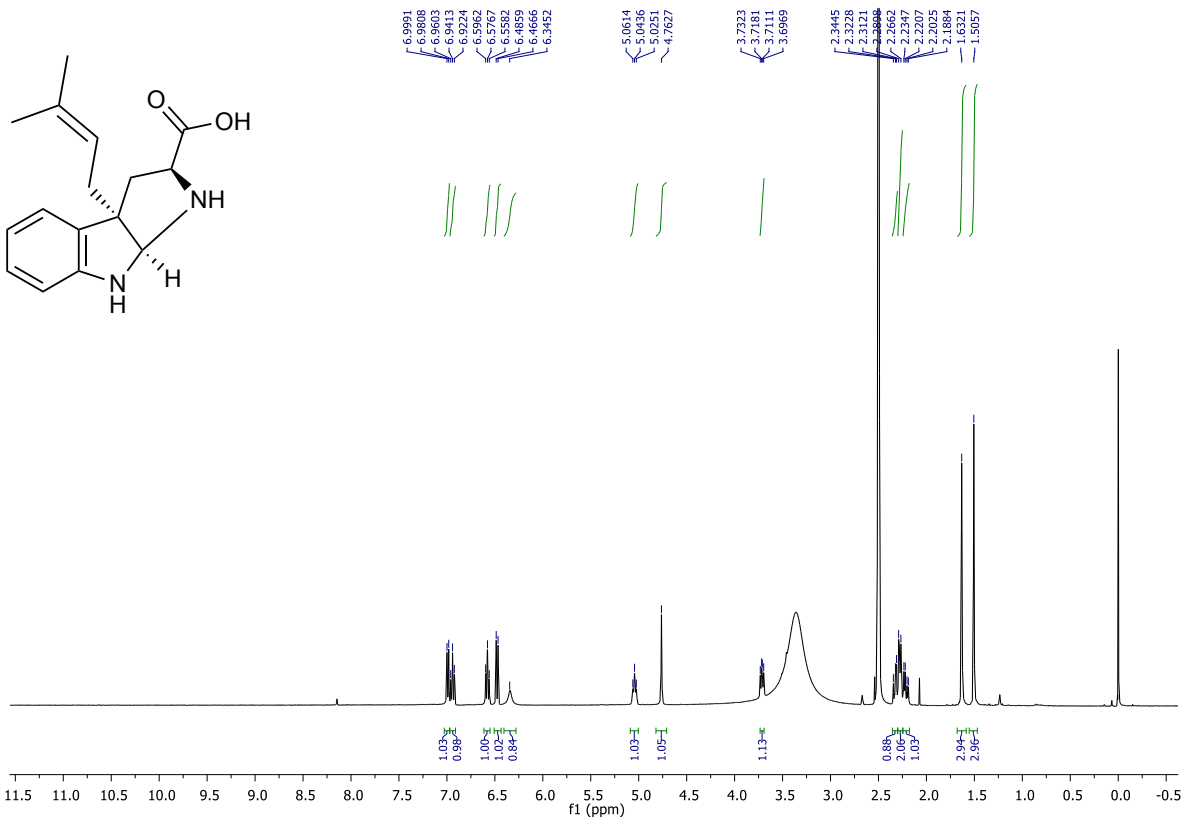

^{1}H NMR spectrum (*d*$_6$–DMSO, 400 MHz) of (2*S*)-3a-(3-methylbut-2-en-1-yl)-1,2,3,3a,8,8a-hexahydropyrrolo[2,3-b]indole-2-carboxylic acid (*d*$_6$–DMSO) **3b**.

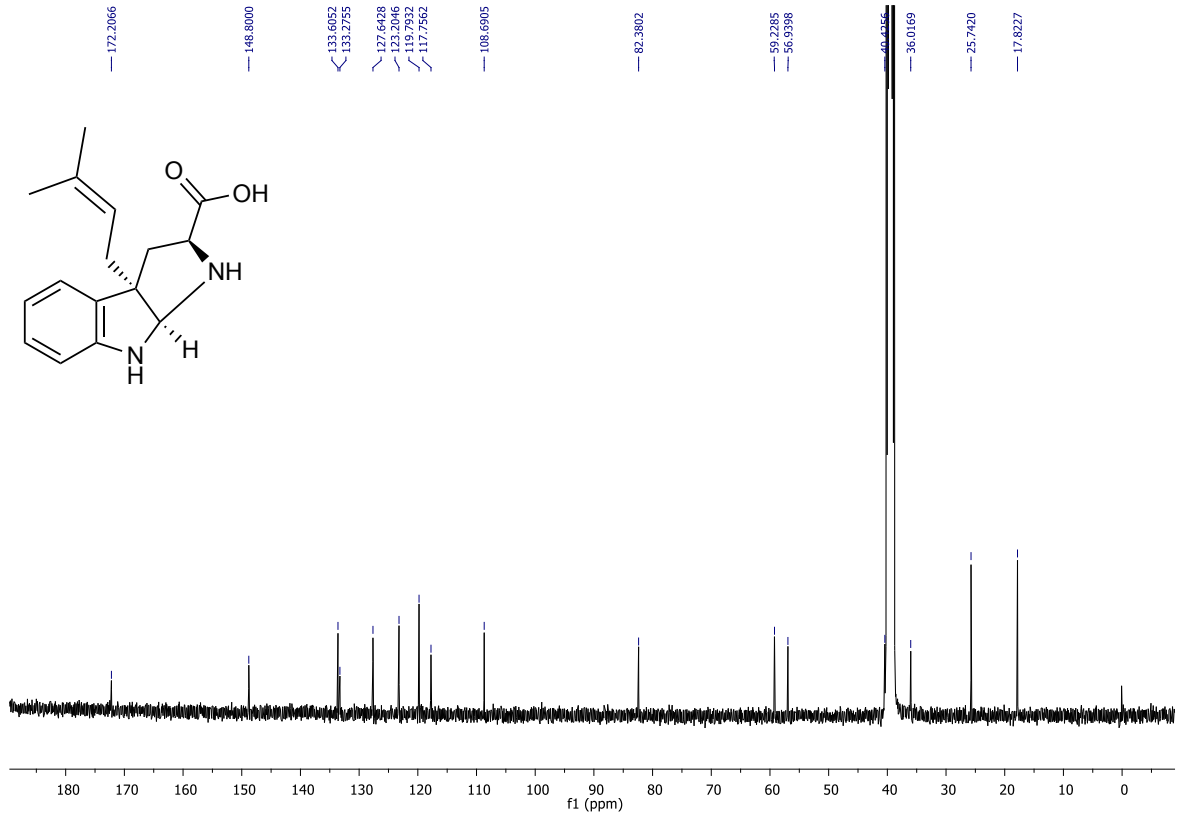

^{13}C NMR spectrum (*d*$_6$–DMSO, 100 MHz) of (2*S*)-3a-(3-methylbut-2-en-1-yl)-1,2,3,3a,8,8a-hexahydropyrrolo[2,3-b]indole-2-carboxylic acid (*d*$_6$–DMSO) **3b**.

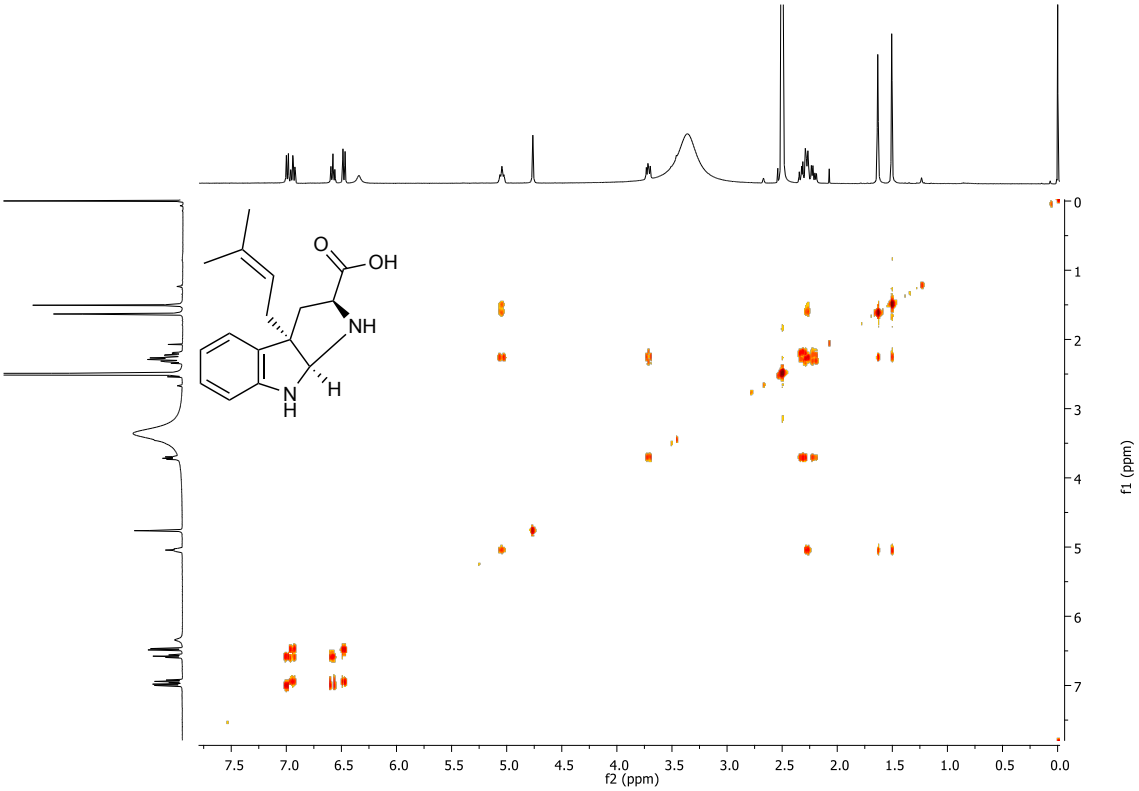

^{1}H-^{1}H COSY NMR spectrum (*d*$_{6}$–DMSO, 400 MHz) of (2*S*)-3a-(3-methylbut-2-en-1-yl)-1,2,3,3a,8,8a-hexahydropyrrolo[2,3-b]indole-2-carboxylic acid (*d*$_{6}$–DMSO) **3b**.

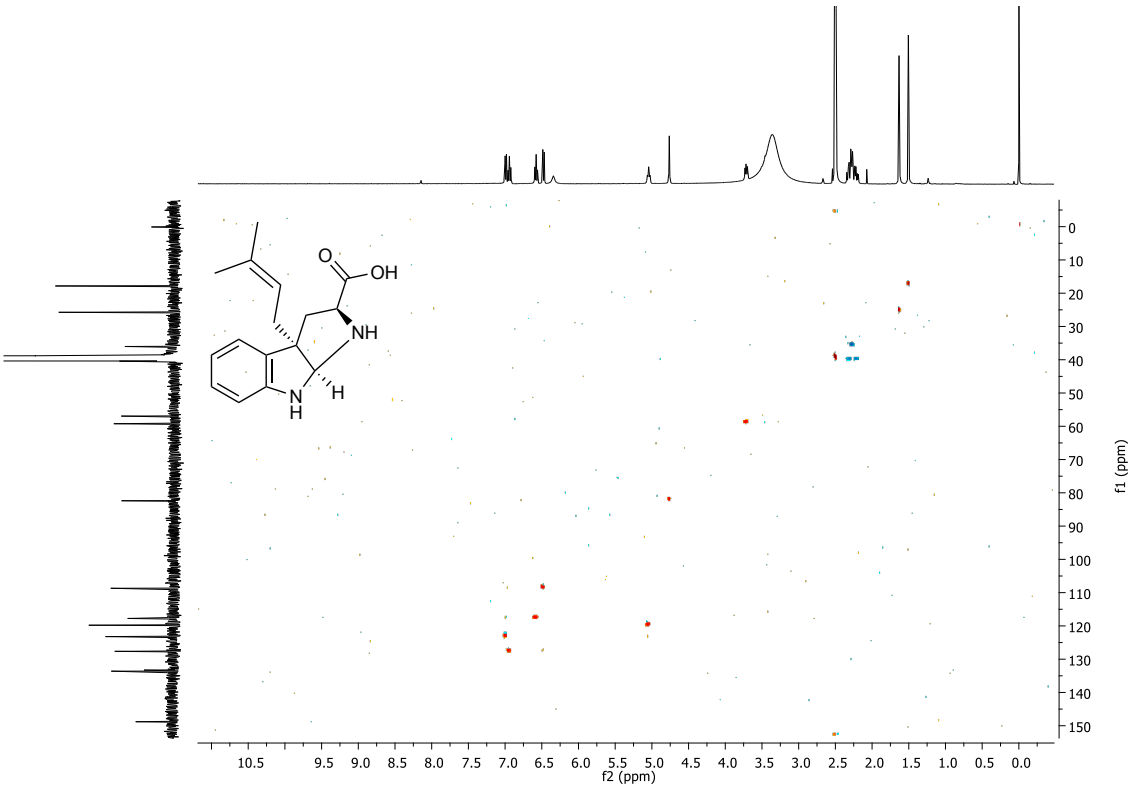

^{1}H -^{13}C HSQC spectrum (DMSO-*d6*, 400 MHz) of (2*S*)-3a-(3-methylbut-2-en-1-yl)-1,2,3,3a,8,8a-hexahydropyrrolo[2,3-b]indole-2-carboxylic acid (*d*$_{6}$–DMSO) **3b**.

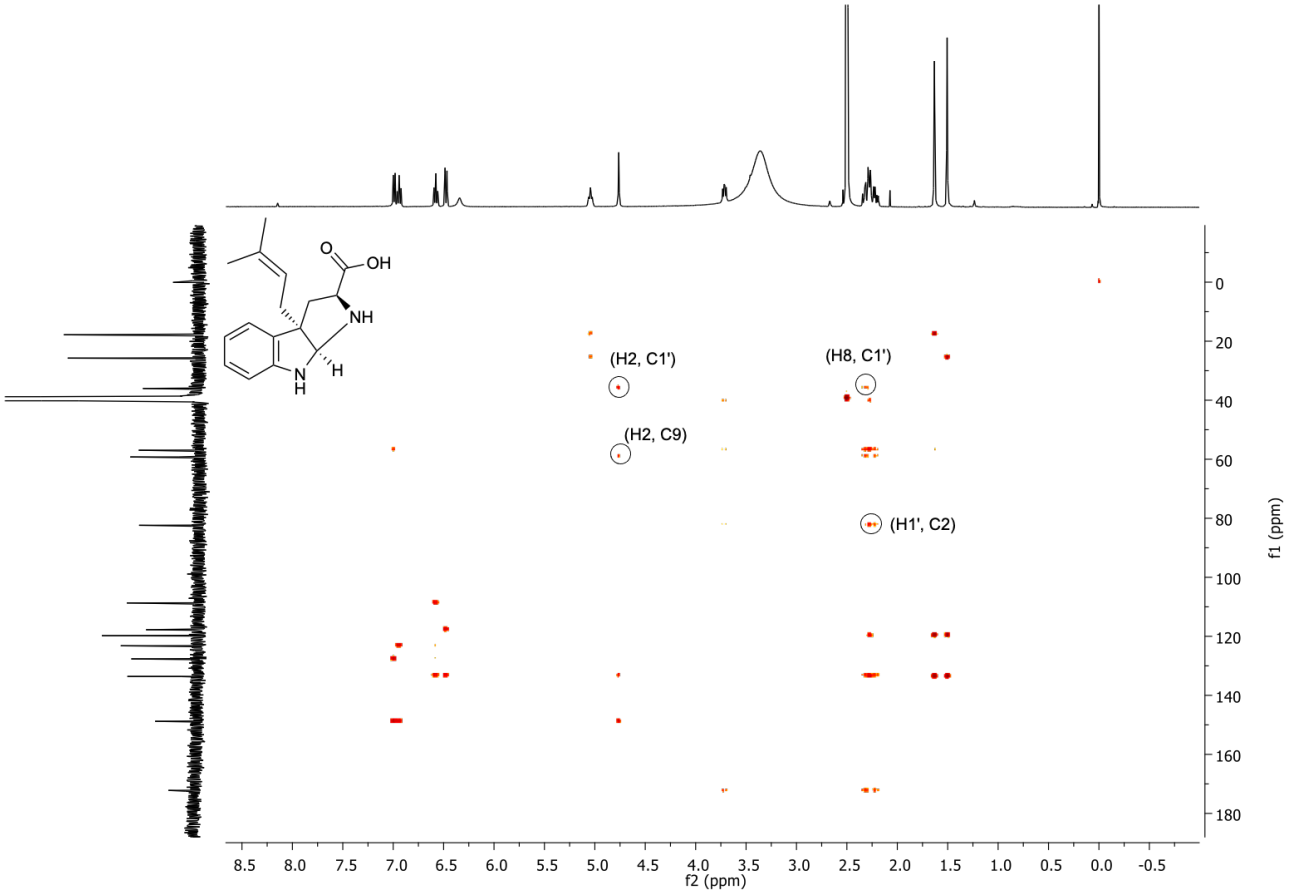

^{1}H-^{13}C HMBC NMR spectrum (*d*$_6$–DMSO, 400 MHz) of (2*S*)-3a-(3-methylbut-2-en-1-yl)-1,2,3,3a,8,8a-hexahydropyrrolo[2,3-b]indole-2-carboxylic acid (*d*$_6$–DMSO) **3b**. Significant correlations are highlighted.

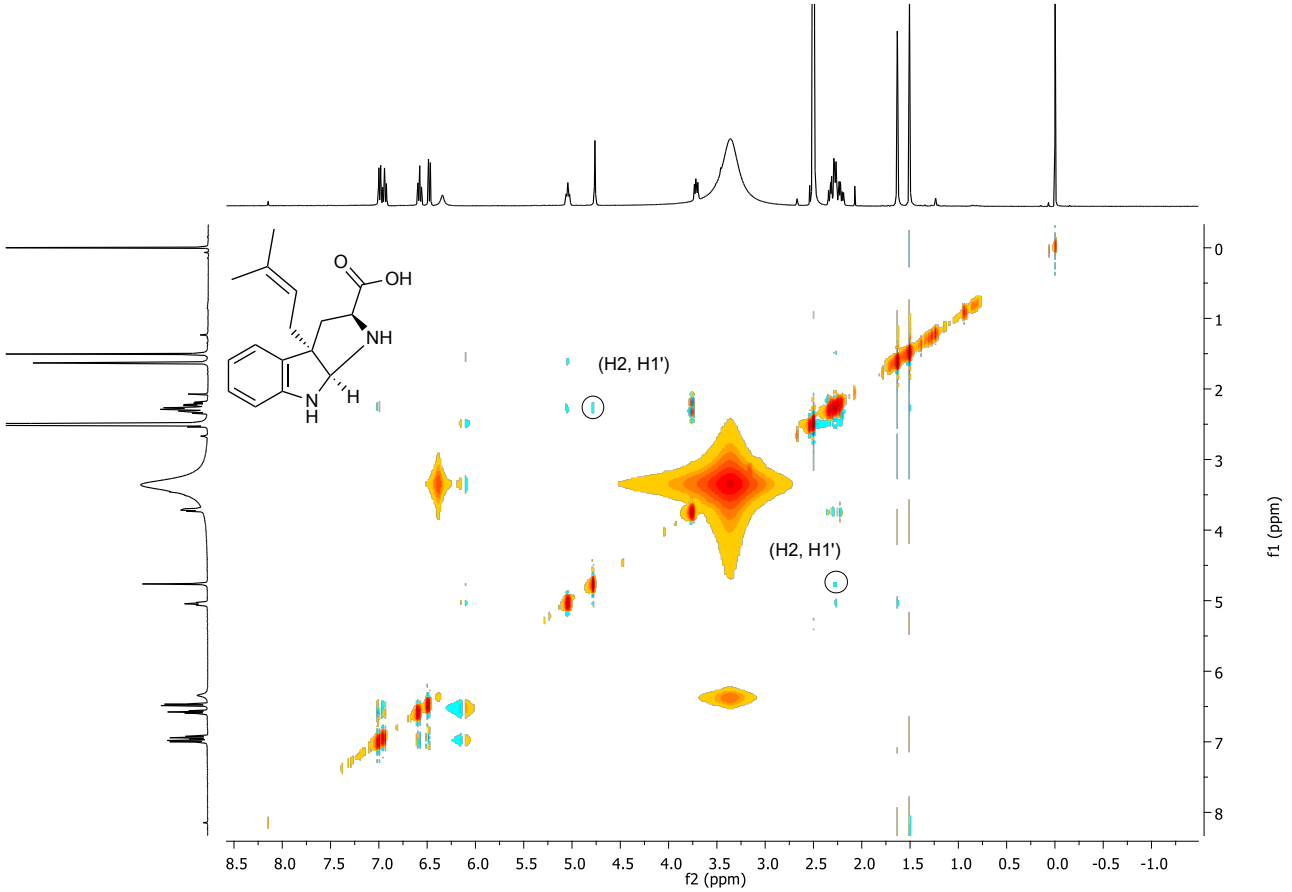

^{1}H-^{1}H NOESY NMR spectrum (d_6–DMSO, 400 MHz) of (2*S*)-3a-(3-methylbut-2-en-1-yl)-1,2,3,3a,8,8a-hexahydropyrrolo[2,3-b]indole-2-carboxylic acid (d_6–DMSO) **3b**. One significant correlation is highlighted.

Analysis Info

Analysis Name	D:\Data\Elshahawi\NMupparapu\LC MS Data\NM-III-82A-1B-2_RE2_1_4637.d	Acquisition Date	2/16/2022 3:13:07 PM
Method	LC_15min_MsMs_M2.m	Operator	Demo User
Sample Name	NM-III-82A-1B-2	Instrument	impact II
Comment			

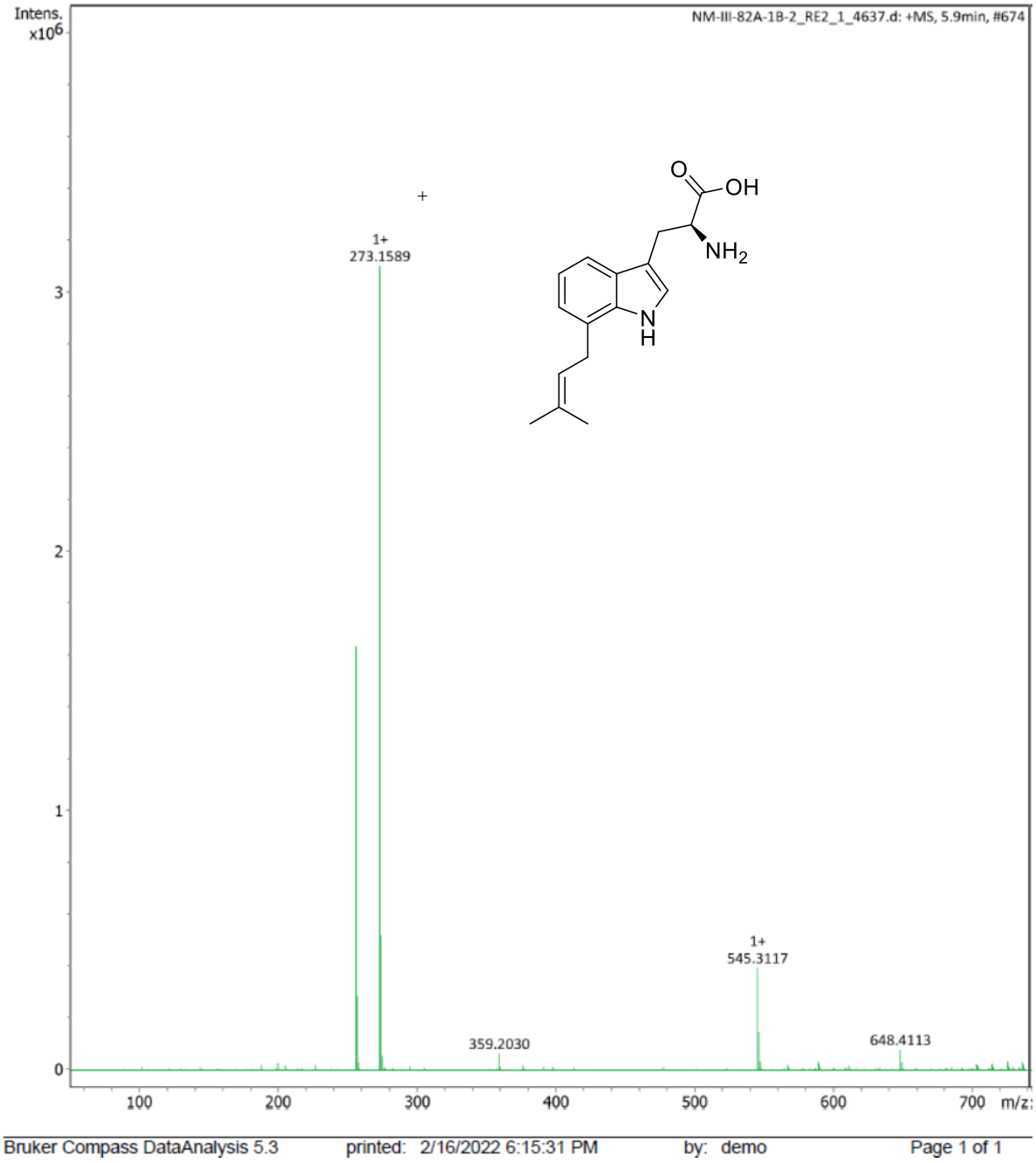

Bruker Compass DataAnalysis 5.3 printed: 2/16/2022 6:15:31 PM by: demo Page 1 of 1

LC-HR-ESI-MS of (*S*)-2-amino-3-(7-(3-methylbut-2-en-1-yl)-1*H*-indol-3-yl)propanoic acid **3c**.

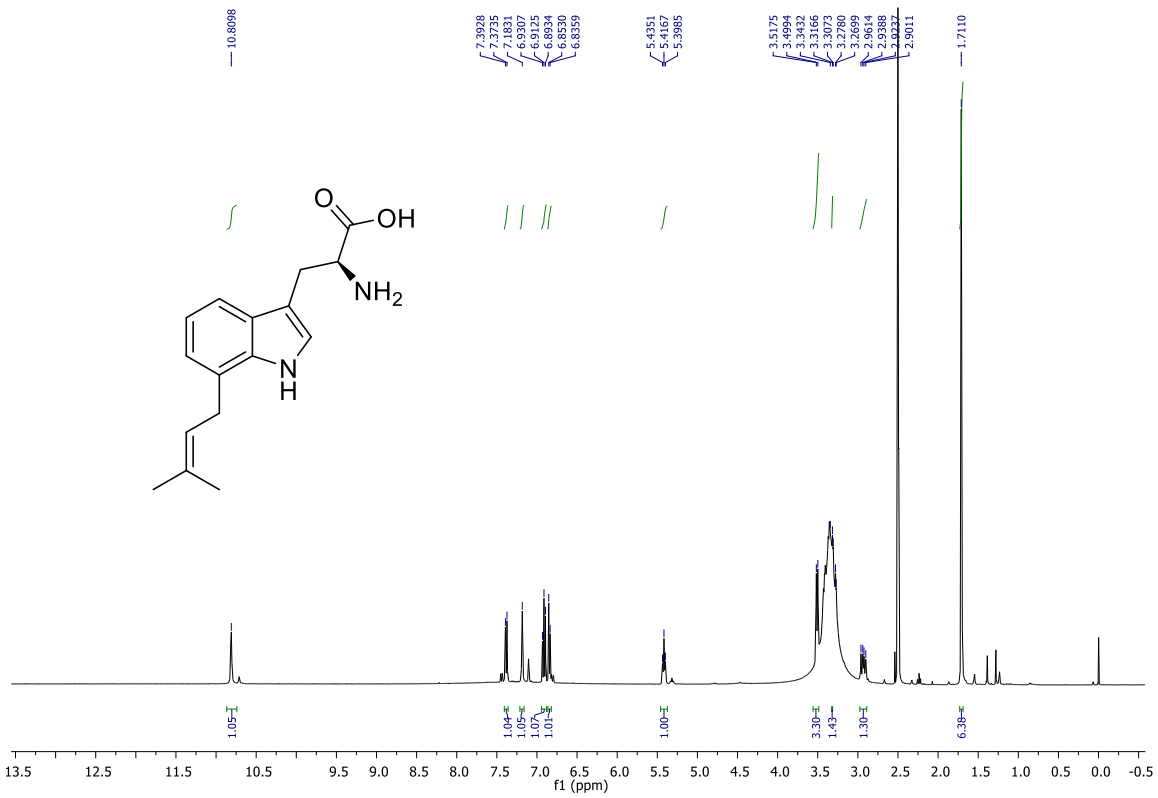

^{1}H NMR spectrum (d_6–DMSO, 400 MHz) of (*S*)-2-amino-3-(7-(3-methylbut-2-en-1-yl)-1*H*-indol-3-yl)propanoic acid **3c**.

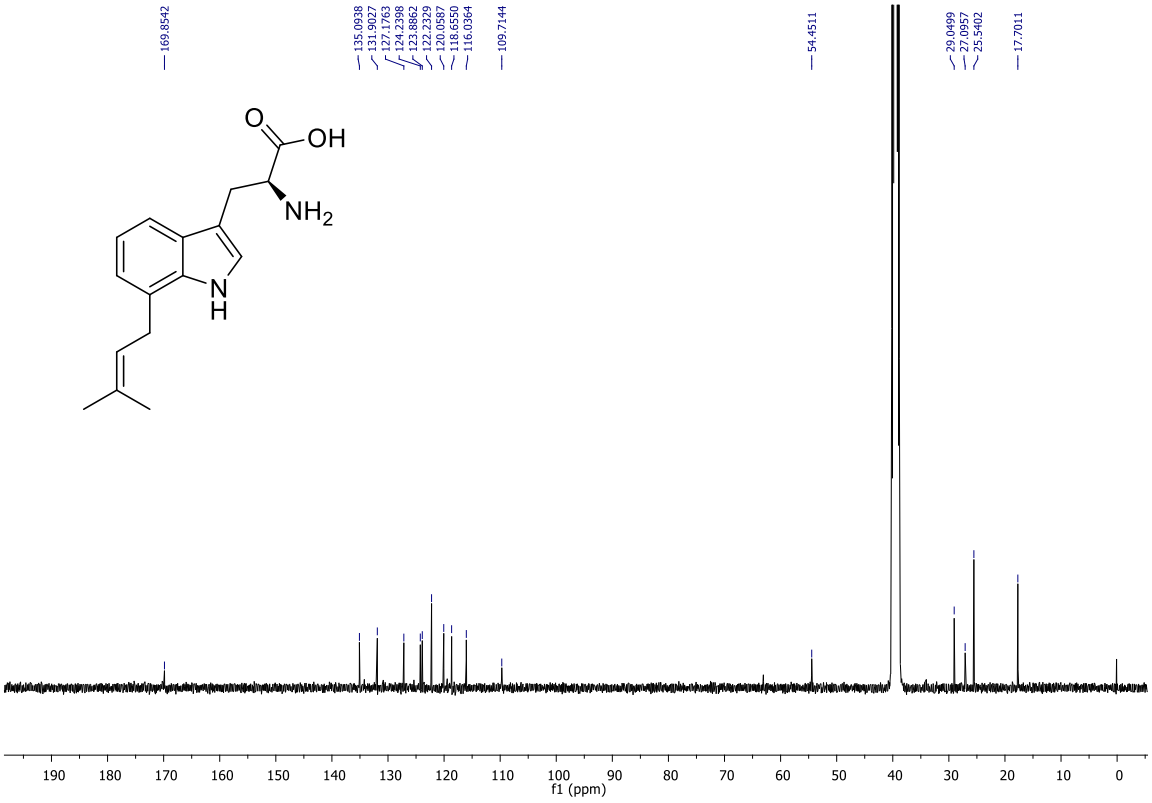

^{13}C NMR spectrum (d_6–DMSO, 100 MHz) of (*S*)-2-amino-3-(7-(3-methylbut-2-en-1-yl)-1*H*-indol-3-yl)propanoic acid **3c**.

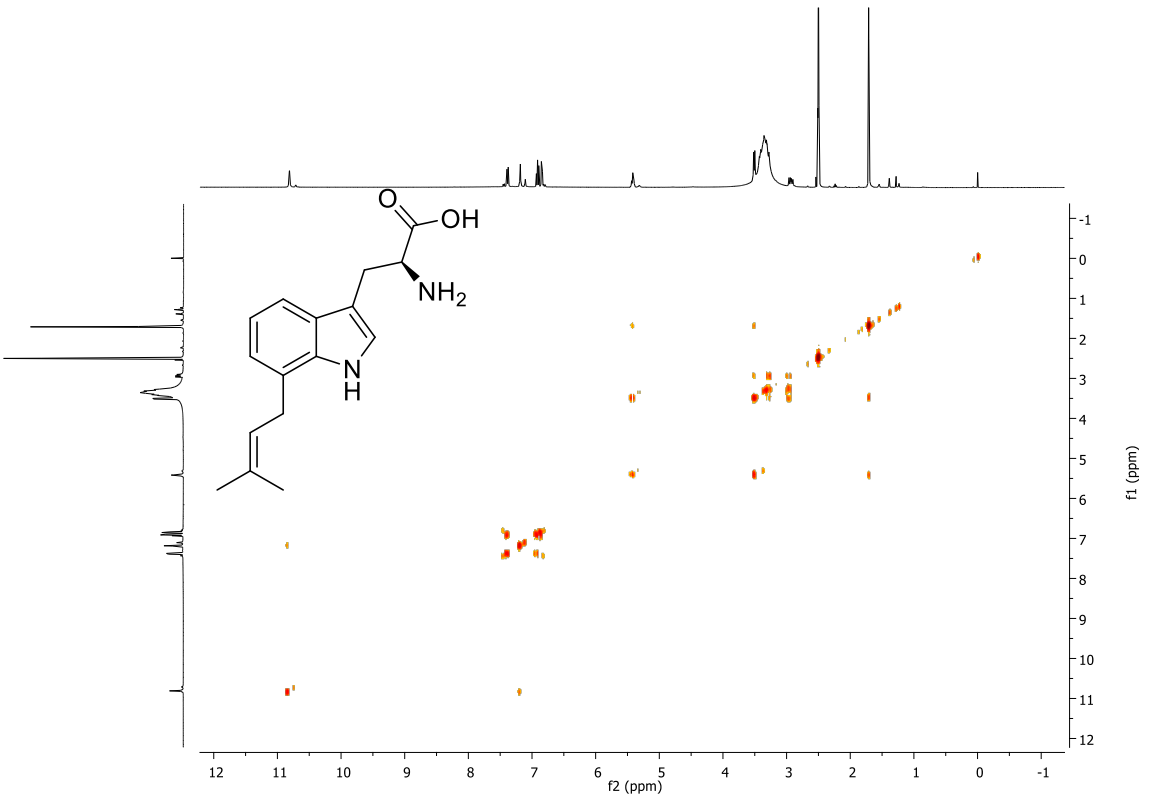

^{1}H-^{1}H COSY NMR spectrum (*d*$_{6}$–DMSO, 400 MHz) of (*S*)-2-amino-3-(7-(3-methylbut-2-en-1-yl)-1*H*-indol-3-yl)propanoic acid **3c**.

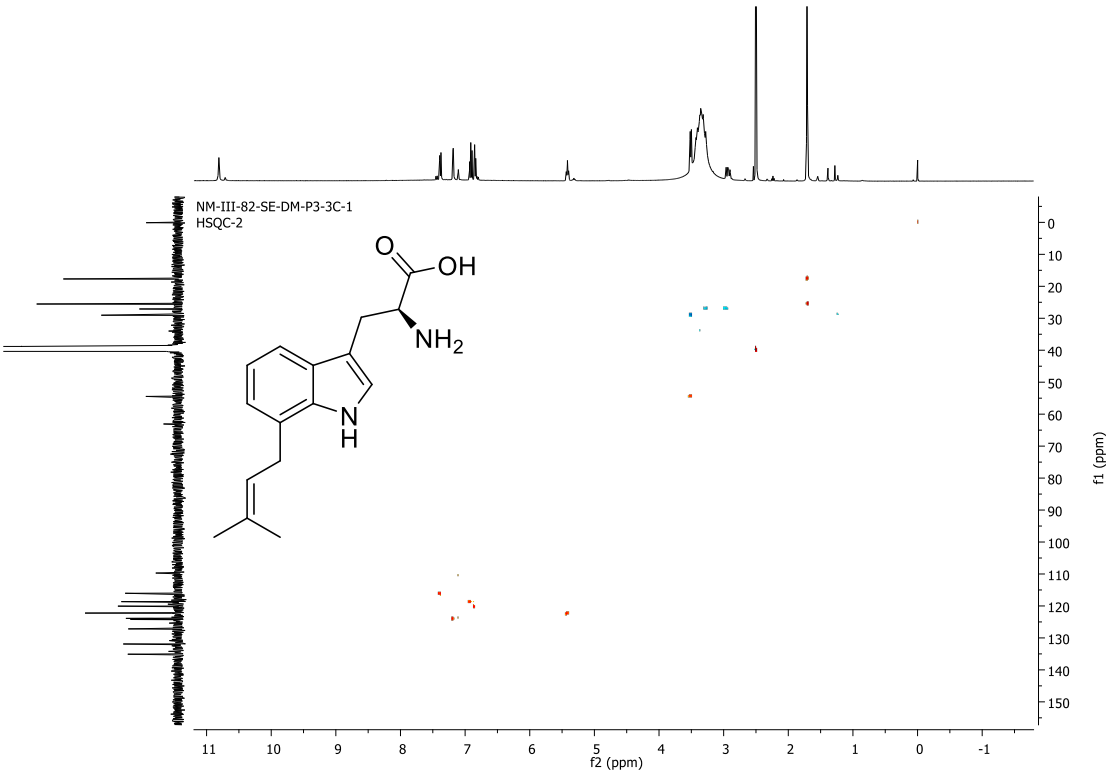

^{1}H -^{13}C HSQC spectrum (DMSO-*d6*, 400 MHz) of (*S*)-2-amino-3-(7-(3-methylbut-2-en-1-yl)-1*H*-indol-3-yl)propanoic acid **3c**.

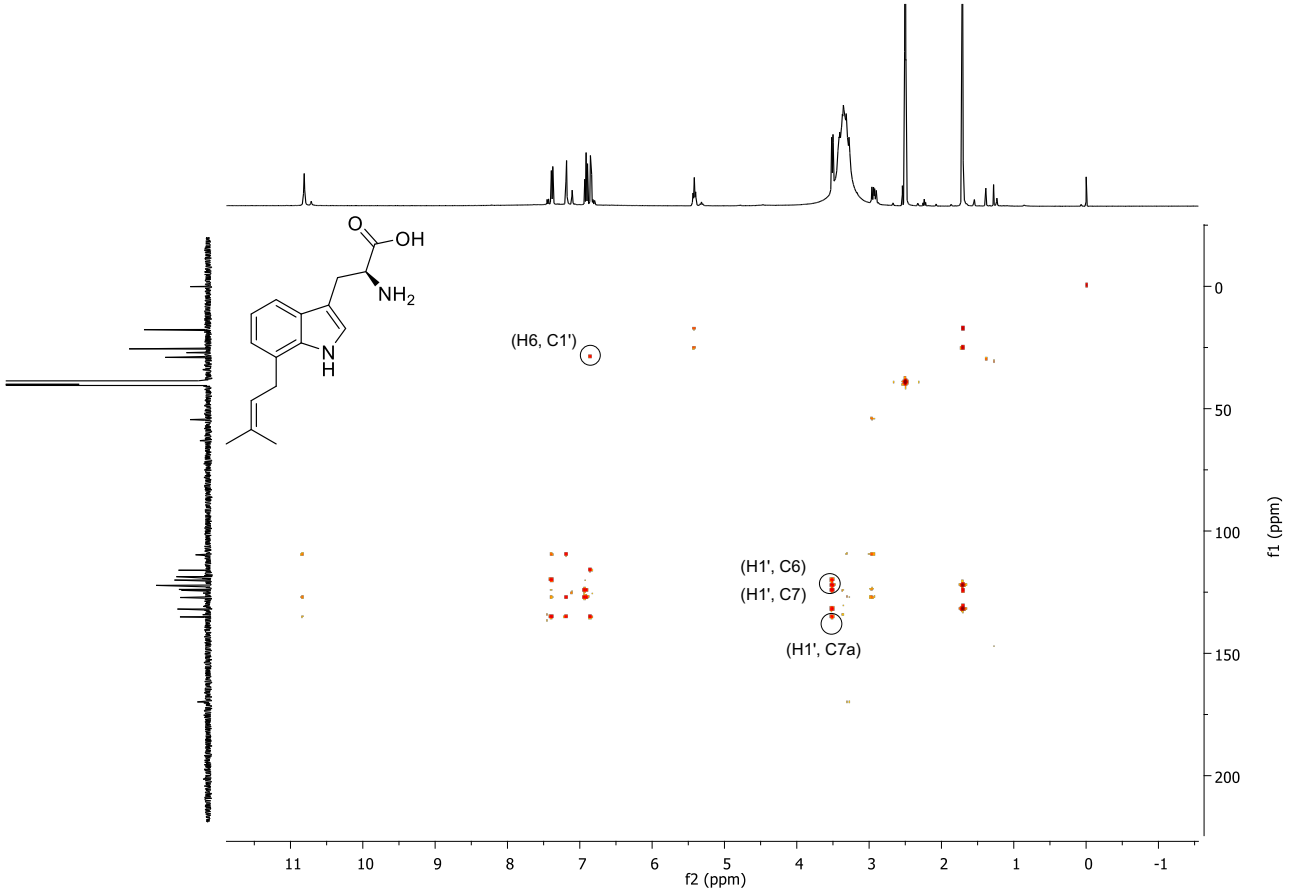

^{1}H-^{13}C HMBC NMR spectrum (d_6–DMSO, 400 MHz) of (*S*)-2-amino-3-(7-(3-methylbut-2-en-1-yl)-1*H*-indol-3-yl)propanoic acid **3c**. Significant correlations are highlighted.

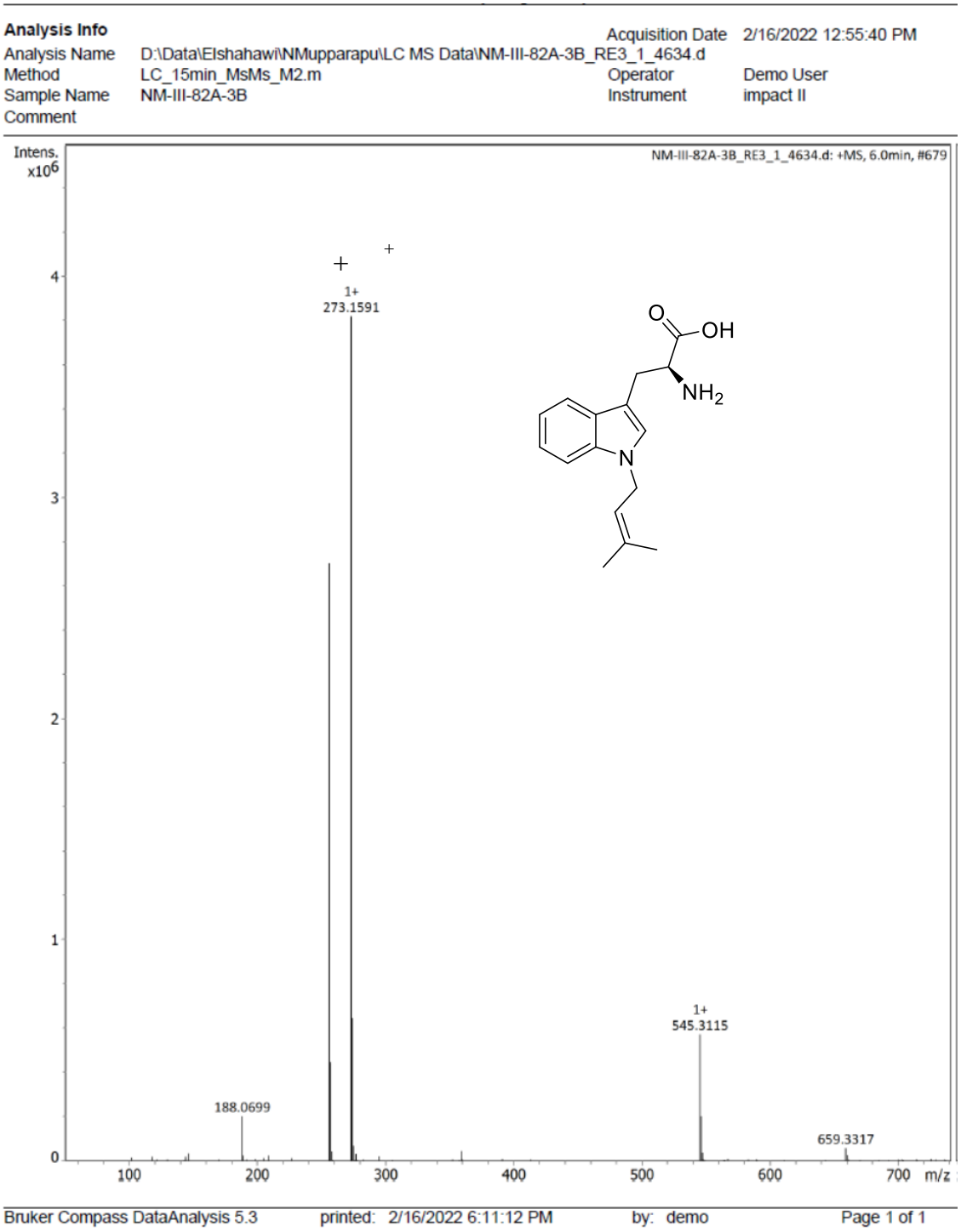

LC-HR-ESI-MS of 1-(3-methylbut-2-en-1-yl)-L-tryptophan **3d**.

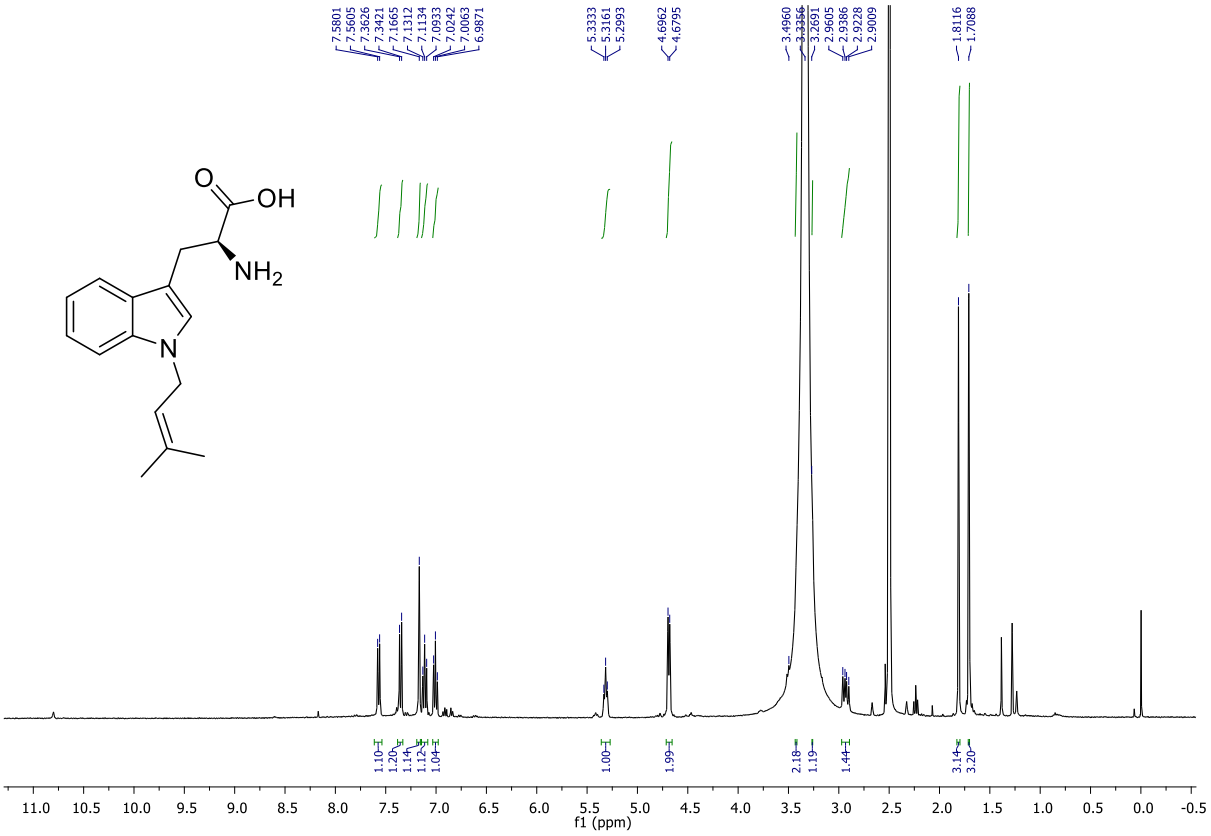

^{1}H NMR spectrum (d_6–DMSO, 400 MHz) of 1-(3-methylbut-2-en-1-yl)-L-tryptophan **3d**.

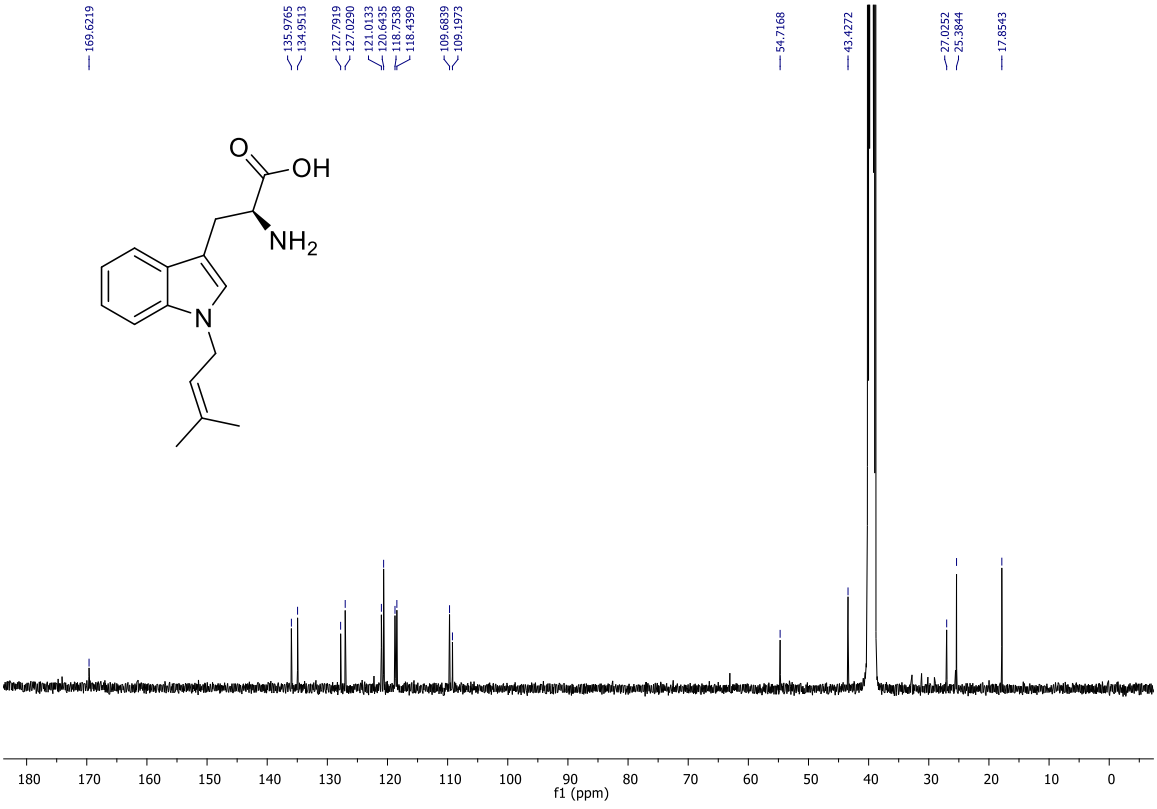

^{13}C NMR spectrum (d_6–DMSO, 100 MHz) of 1-(3-methylbut-2-en-1-yl)-L-tryptophan **3d**.

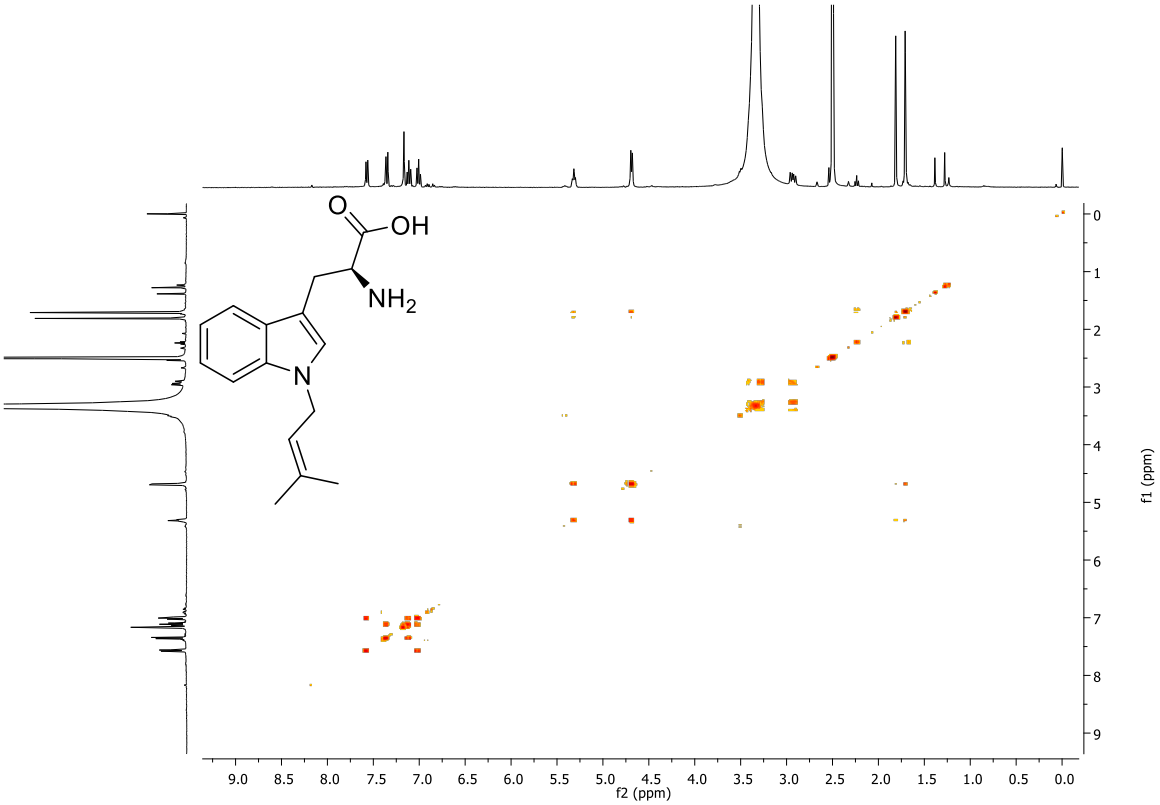

^{1}H-^{1}H COSY NMR spectrum (d_6–DMSO, 400 MHz) of 1-(3-methylbut-2-en-1-yl)-L-tryptophan **3d**.

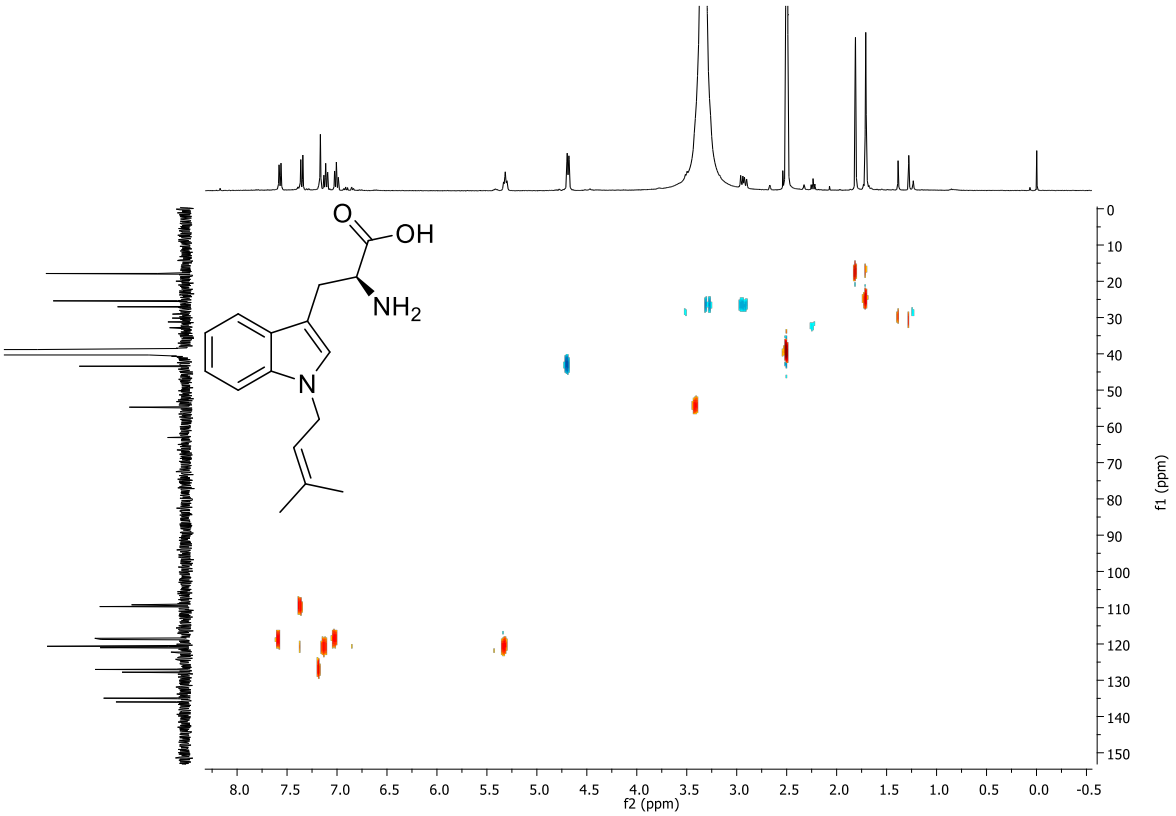

^{1}H -^{13}C HSQC spectrum (DMSO-*d6*, 400 MHz) of 1-(3-methylbut-2-en-1-yl)-L-tryptophan **3d**.

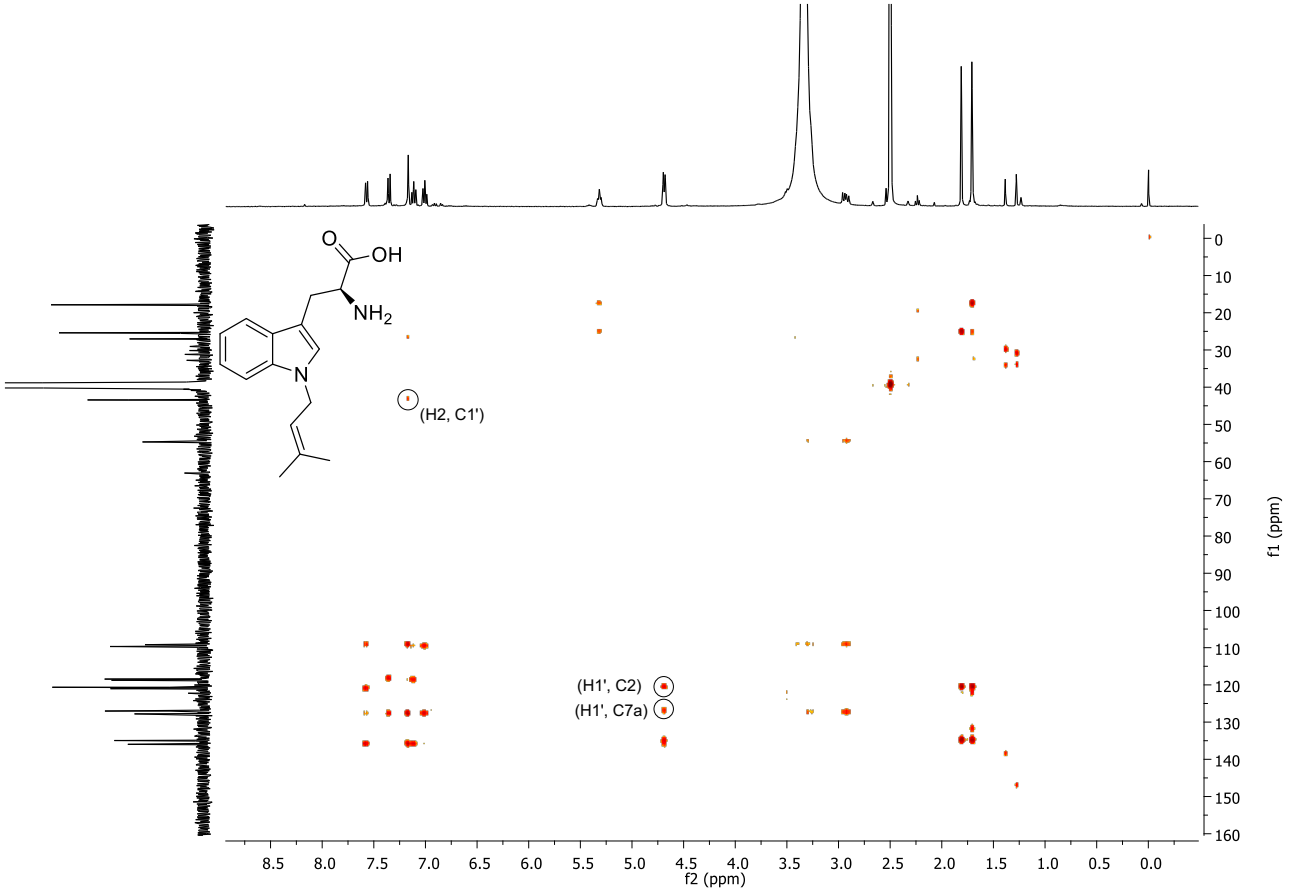

^{1}H-^{13}C HMBC NMR spectrum (*d*$_{6}$–DMSO, 400 MHz) of 1-(3-methylbut-2-en-1-yl)-L-tryptophan **3d**. Significant correlations are highlighted.